united nations educational, scientific and cultural organization

international atomic energy agency

**abdus salam**
international centre for theoretical physics

H4.SMR/1241-19

"Workshop on Three-Dimensional Modelling of Seismic Waves Generation and their Propagation"

25 September - 6 October 2000

# LOCAL EARTHQUAKE TOMOGRAPHY (LET) AND COLLISIONAL MOUNTAIN BUILDING

*F. WU*

**State University of New York**
**Dept. of Geological Sciences**
**New York, Binghampton**
**U.S.A.**

strada costiera, 11 - 34014 trieste italy - tel. +39 0402240111 fax +39 040224163 - sci_info@ictp.trieste.it - www.ictp.trieste.it

# Local Earthquake Tomography (LET) and Collisional Mountain Building

by

Francis T. Wu

# Requirements

- Well-distributed earthquakes
- Dense network
- Narrowband or broadband?

LET is a travel time tomography. For each earthquake
And station pair the travel time is

$$t = \tau + \int_{l[u(\mathbf{r})]} u(\mathbf{r})\,dl$$

Here $\tau$ is the starting time and is actually an unknown since a change in location will affect the time it takes to travel to the station and the origin time. The integral is performed along the ray path with slowness (reciprocal of velocity) field vary along the path. In the simple earthquake location problem $u(\mathbf{r})$ is assumed to be known but in reality we don't know and is for LET to find out.

# Steps to implement LET

- A particular choice for parameterizing a model
- Technique for calculating travel time and ray path.
- The treatment of hypocenter-ray path coupling
- The method of inversion
- An assessment of solution quality
- The use of S waves

In matrix form:

$$r_i = H_i \Delta h_i + M_i \Delta m$$

Three separate research groups recognized around 1980 that the earthquake location part and the velocity model part can be separated, based on a matrix theorem:

$$U_0^T r_i = U_0^T M_i \Delta m$$

# Tomography version 2

- Rau and Wu (1995) used 4 years of the Taiwan seismic network data
- About 1000 events were selected
- Based on Thurber's methodology
- Blocks of ~30km with velocity gradient inside

## High Resolution Tomography of Taiwan

Francis T. Wu
State University of New York
Binghamton, New York
USA

Lecture Notes for "5th Workshop on Three-Dimensional Modeling of Seismic Waves Generation, Propagation and Their Inversion", 2000.

Introduction

1. Previous tomography of Taiwan

The first tomographic image of Taiwan was obtained by Roecker et. al. (1987) using 15 years of local earthquake data from the Taiwan Telemetered Seismic Network (TTSN – operated by the Institute of Earth Sciences, Academia Sinica, 1971-1990) and also temporary stations set up for various monitoring purposes. The combined spacing of TTSN and other was rather uneven (varies from about 10-70 km) of TTSN the block size adopted was 30 km. The main features that appeared in the image is the relatively high velocity at shallow depths (0-15 km) and relatively low velocity at depth range of 15-30 km in parts of the Central Range. In 1990 TTSN was replaced by a denser, digitally recording network; with a total of 73 stations the spacing of the stations ranges from 10-30 km. The enhanced dynamic range and frequency response led to a rapidly growing dataset. Rau and Wu (1995) used only four years of data to select a set of 1197 earthquakes for the imaging of both the crust and parts of the upper mantle the intermediate earthquakes in the Taiwan area illuminated. Since then a number of efforts have been made in imaging. Several papers used the same methodology as Rau and Wu (1995) and obtained similar results. Ma and Zhao constrained the Moho depth using Zhao's program. Since the Moho depth was fixed, the images did not see a root. The chief features imaged by Rau and Wu (1995) and the ensuing works included a substantial root under the high mountain, somewhat deeper in the north and decreasing slowly toward the south, the high velocity zone associated with the dipping subduction structures under northern Taiwan, and so on.

2. Tectonics and the questions that detailed tomography can address

Taiwan is situated on the boundary between the Eurasian and the Philippine Sea plates. While it is agreed by most that it is in a collision zone and the ensuing shortening led to the formation a mountain range exactly how the mountains were built is still being argued. Suppe (1987) presented the view that a detachment fault or a decollement underlie the whole island and the mountain was built by advancing the Philippine Sea plate against the Tertiary sediments in a "critically tapered" wedge. It is "thin-skinned" in that the detachment fault was shallow dipping (with a dip angle of 6 degree or so) and the deepest part of the crust such decollement would reach is less than 15 km. The deformation of the sediments in the wedge is not that different from the deformation of trench sediments in an accretionary wedge. In fact the Taiwan mountain range is considered a continuation of the Northern Luzon subduction, except under Taiwan the Eurasian continental lithosphere is assumed to the subducting, instead of the quasi-continental lithosphere of the South China Sea.

Wu et. al. (1997) concluded on the basis of the tomography by Rau and Wu (1995) and other observations that collision in Taiwan involves the deformation throughout the lithospheres on both sides of the boundary. They interpreted the Taiwan orogeny as a three-dimensional structure, not a simply north-to-south propagation of a deformation wedge. More details of this and other hypotheses can be found in the accompanying reprint by Wu et. al. (1997).

Recent teleseismic tomography of Bijward shows a a high velocity zone at the depth range of 200-400 km. Lallemand (2000) interpreted this as a signature for a subduction zone; it is thought to be inactive and perhaps fossilized. Lacking associated seismicity this zone could also be interpreted as a result of crustal thickening (Molnar et. al., 2000; later discussion). Future tomography using teleseismic arrivals recorded by the Taiwan Seismic Network (operated by Central Weather Bureau) can resolve similar questions under Taiwan.

Since the spatial distribution of seismicity is a function of time and, with fixed station, seismicity controls the illumination of different parts of the crust. With more events one could select the dataset more critically. Thus it is worthwhile to perform tomography every few years in the region even though the station configuration has not changed. But it is especially worthwhile in this case because we can use a relatively new methodology by Benz (see Benz et. al., 1995) that is particularly suited for using large dataset and for obtaining images of higher resolution. The method is based on the ray-tracing method of Povin and Lecomte (1991). Solving the Eikonal equation in a finite-difference grid of rectangular, constant velocity cells, the travel time wavefront is estimated. By starting the ray-tracing from each station, the set of rays needed to connect up with the events can be calculated efficiently. With such method it is practical to use blocks of 5km x 5 km x 2km (in the x, y and z directions) in Taiwan. Besides the ray-tracing algorithm also allows sudden velocity change between grids, allowing head waves to be included.

Some of the results are shown in grey-scale illustrations in Figures 1 and 2. Although the crustal root of the mountains can still be clearly discerned and the changes in crustal thickness in the north-south direction is also clear, in the new images the asymmetry of the root becomes much more pronounced, the intracrustal velocity distribution clearer and more interestingly rather high velocities are seen at the top of the subduction zone, around the bend. The nature of this zone is still being explored. The grey-scale figures cannot show all the features in the tomographic images; but a paper is being prepared for presenting the results.

References

Rau and Wu, 1995. Included in this package.

Wu, Rau and Salzberg, 1997. Included in this package.

Suppe, 1987, see reference in Wu et. al., 1997.

Podvin, P. and I. Lecomte, 1991. Finite difference computation of traveltimes in very contrasted velocity models: a massively parallel approach and its associated tools, Geophys. J. Int., vol. 105, 271-284.

Roecker, S.W., Y.H. Yeh, and Y.B. Tsai, 1987. Three-dimensional P and S wave velocity structures beneath Taiwan: deep structure beneath an arc-continent collision, J. Geolphys. Res., vol. 92, 10,547-10570.

Thurber, C.H. 1993. Local earthquake Tomography: velocities and Vp/Vs – Theory, in Iyer and Hirhara (editors) Seismic Tomography: Theory and Practice, Chapman and Hall, London. [This is a very thorough discussion of Local Earthquake Tomography.]

Reprinted from

TECTONOPHYSICS

INTERNATIONAL JOURNAL OF GEOTECTONICS AND THE GEOLOGY AND PHYSICS OF THE INTERIOR OF THE EARTH

Tectonophysics 274 (1997) 191–220

# Taiwan orogeny: thin-skinned or lithospheric collision?

Francis T. Wu *, Ruey-Juin Rau, David Salzberg

*Department of Geological Sciences, State University of New York, Binghamton, NY 13902, USA*

Accepted 16 December 1996

ELSEVIER

**Scope of the journal**
*Tectonophysics* is an international medium for the publication of original studies and comprehensive reviews in the field of geotectonics and the geology and physics of the earth's crust and interior. The editors will endeavour to maintain a high scientific level and it is hoped that with its international coverage the journal will contribute to the sound development of this field.

*(Text continued on inside back cover)*



ELSEVIER

TECTONOPHYSICS

Tectonophysics 274 (1997) 191–220

# Taiwan orogeny: thin-skinned or lithospheric collision?

Francis T. Wu *, Ruey-Juin Rau, David Salzberg

*Department of Geological Sciences, State University of New York, Binghamton, NY 13902, USA*

Accepted 16 December 1996

## Abstract

The Taiwan orogeny is young and presently very active. It provides an excellent environment for studying ongoing orogenic processes, especially since the region is monitored intensively with dense seismological and geodetic networks, and new studies aiming at deciphering shallow and deep structures in and around Taiwan have been recently conducted or are being planned. The available data can be used continually to test critically hypotheses of the Taiwan orogeny. Hypotheses dealing with the mechanics of mountain building are basic to the understanding of Taiwan orogeny and are particularly amenable to testing. The widely cited 'thin-skinned tectonics' hypothesis was formulated to explain mainly the geologic and relatively shallow (<10 km) seismic data. In various forms of this hypothesis, the mountain building involves the deformation of ready-to-fail (Tertiary) sediments in a thin (<20 km at the deepest point) wedge deformed by the advancing Philippine Sea plate; the Eurasian plate is assumed to subduct the Philippine Sea plate with the Taiwan orogenic belt on top as an accretionary wedge. We tested this hypothesis against newly acquired seismological and geophysical data and found it to be largely inadequate as a model for Taiwan orogeny, because the evidence for the participation of the lower crust and even the upper mantle in the orogeny is very strong. Rather than the result of deforming a thin wedge, the formation of the Central Range is shown to include the thickening of crust as well as the extrusion of mid- to lower crustal high-velocity materials to shallow depth. Seismicity and focal mechanisms demonstrate that significant deformation is taking place at depths far below what the thin-skinned tectonics hypothesis predicts. As an alternative, the lithospheric collision hypothesis is proposed. In this model the Eurasian and the Philippine Sea plates are colliding at least down to a depth of 60 km. This hypothesis involves not only greater depth but also greater lateral extent. It accounts for the formation of the deep-rooted Central Range on the Eurasian side, as well as the shortening and thickening of the margin of the Philippine Sea plate near Taiwan. It also asserts that the Central Range was built mainly under ductile conditions, while in the Western Foothills area, the deformation involves the whole brittle–ductile–brittle–ductile sandwiched crust and upper mantle. Furthermore, it is asserted that the collision effect is transmitted to the Taiwan Strait resulting in normal faulting striking perpendicular to the trend of Taiwan. Among the implications of this hypothesis some can be readily subjected to falsification. By critically evaluating the components and accepting or rejecting them, our understanding of the Taiwan orogeny in particular and mountain building in general can be improved.

*Keywords:* orogeny; Taiwan; collision; lithospheric structures; crustal rheology; tectonic model

* Corresponding author. E-mail: wu@sunquakes.geol.binghamton.edu.

0040-1951/97/$17.00 © 1997 Elsevier Science B.V. All rights reserved.
*PII* S0040-1951(96)00304-6

## 1. Introduction

The Taiwan orogeny is geologically young; while estimates from changes in the rate of sedimentation and paleomagnetic evidence all point to a starting time of about 4 million years ago (Suppe, 1984; Lee et al., 1991), the fission-track dating puts the most rapid uplifting within the last 1 million years (Tsao et al., 1992). The rapid rate of deformation detected geodetically on the island and the high level of seismicity in and around Taiwan demonstrate its present day activity (Wu et al., 1989; Yu and Chen, 1994). It is clear that the continuous convergence of the northern part of the Luzon Arc, on the Philippine Sea plate and the Asian continental shelf was responsible for the creation of the island and the mountain ranges (Fig. 1). Because the Luzon Arc and the shelf are not parallel, the collision started near Hualien, about 4 million years ago, and moved progressively southward to reach Taitung about 1 million years ago (Lee et al., 1991); therefore a time-slice of the orogeny can be obtained by following a longitudinal profile from Hualien to Taitung, a result of diachronous collision (Suppe, 1987). That Taiwan is a product of an arc–continent collision was first recognized by Chai (1972), and since then the orogenic evolution and the plate tectonic settings have been explored by many investigators (see, for example, Wu, 1978; Biq, 1981; Suppe, 1981, 1984, 1987; Davis et al., 1983; Tsai, 1986). The ultimate aim in the study of Taiwan orogeny must be the modeling of the evolution of the geological processes underlying the orogeny. Such tasks in geosciences are inherently difficult, due to the lack of continuous geologic records and direct knowledge of the geologic processes at depth. But being one of the youngest mountain ranges on earth, the Taiwan orogeny is more amenable to detailed modeling than ones that have long ceased to be active. Here the gaps in geological records are not as long, and we are able to probe the ongoing orogenic processes.

In the studies of the Taiwan orogen, the thin-skinned tectonics hypothesis (or model) had played an integrative role. Originating as a model for Appalachian tectonics (Rich, 1934), its application to Taiwan was developed in a series of papers. The development of the basic model commenced with studies of the fold-and-thrust belt of western Taiwan (Suppe, 1976), and was completed through the incorporation of shallow (<10 km) borehole and exploration seismic data (Suppe, 1980, 1981) and the linkage between fold-and-thrust and accretionary wedge (Davis et al., 1983). It has been used frequently, either explicitly or implicitly, as a basis for interpreting the geology of Taiwan and its relation to plate motions near Taiwan (e.g., Teng, 1990; Tsao et al., 1992; Reed et al., 1992). Using the basic model, Dahlen and Barr (1989) and Barr and Dahlen (1989) solved the mechanical and thermal problem of 'critical wedge', a thinly tapered wedge with materials at failure condition. This model gives an essentially two-dimensional view of the island, although the variations in tectonic characteristics along the axis of the island have been largely taken into account by assuming a progressive younging of the collision along the whole length of Taiwan. In such a model a decollement at the base of the thin wedge is an integral part, and in Taiwan it is assumed to coincide with the top of an eastward-subducting Eurasian plate.

The thin-skinned model for Taiwan orogeny was developed when little or no deep crustal information was available. Deep seismic sounding using artificial sources had never been carried out in Taiwan. Until 1991, the quality and quantity of seismological data from natural earthquakes were insufficient for imaging the details of mid- and lower crust. Ideally, the high level of seismicity in the vicinity of Taiwan, occurring in response to the collision-induced stresses, can be utilized as an effective means for studying the orogeny. While the earthquakes, their locations and focal mechanisms, enable us to assess the state of strain, the direction of tectonic stress, the rheological properties of the crustal and upper mantle rocks as well as the plate interactions, the seismic waves generated by these earthquakes can be used to map the seismic velocity structures under the island. With an improved seismic network in place since 1991 (Rau et al., 1996), analyses of high-quality, digital data began to yield detailed 3-D velocity structures and well-constrained focal mechanisms in different parts of the orogen, such that the mechanical response of the crust and upper mantle to the collision stresses can be studied. In addition, our understanding of the orogeny is also aided significantly by the fortuitous occurrence of key earthquakes in the last few years.



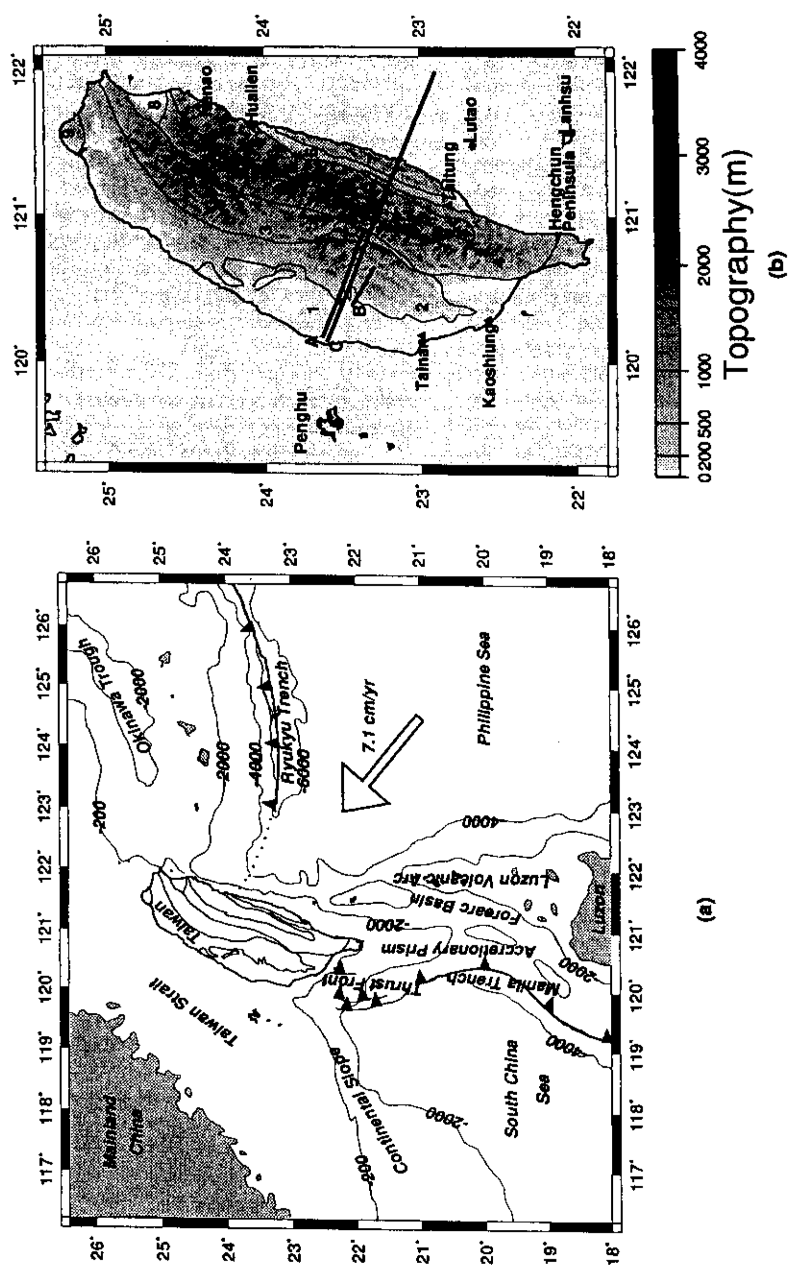


Fig. 1. (a) The overall plate tectonic environment of Taiwan (Rau and Wu, 1995). (b) Main geologic boundaries and physiographic units (Ho, 1988): *1* = western Coastal Plain (Quaternary), *2* = Western Foothills (Plio–Pleistocene), *3* = Hsueshan Range (Eocene–Miocene), *4* = Backbone Range (Eocene–Miocene), *5* = eastern Central Range (Pre-Tertiary), *6* = Longitudinal Valley (Holocene), *7* = Coastal Range (Miocene–Pleistocene), *8* = Ilan Plain (Quaternary), *9* = Tatun volcanic group (Pleistocene). Lines *A*, *B* and *C* are the locations of three schematic cross-sections of Suppe (1987) shown in Fig. 14. The place names mentioned in the main body of the paper are shown in (b).

Furthermore, in addition to the seismic data, the accumulation of other relevant data has accelerated.

With new data available, it may be useful to view the existing hypothesis in the Popperian light (Popper, 1968), i.e., attempts should be made to falsify it. Since the thin-skinned hypothesis was formulated independent of the new data, testing it using such data is suitable. In this paper we shall show that gauged against such data the thin-skinned model of Taiwan orogeny is found to be largely inadequate, mainly because the new data indicate that the orogeny is not limited to the top part of the crust. Instead, the orogeny seems to involve the participation of not only the upper crust, but also the lower crust and uppermost mantle. Also, although the shortening on the Eurasian side of the collision is well-known, the Philippine Sea plate has been considered to be the rigid indentor in the thin-skinned model; but the superposition of the Luzon volcanic arc and the accretionary wedge sediments in the Coastal Range, the high seismicity under the Coastal Range, and the presence of large earthquakes offshore of east Taiwan indicate that significant deformation has occurred on the Philippine Sea side. A recent (September 14, 1994) $M_S = 6.5$ earthquake in the Taiwan Strait even demonstrated that the orogenic effect has propagated to the area west of Taiwan. Thus, based mainly on the new seismic imaging and the distribution of earthquakes in the crust and upper mantle, and incorporating geologic and other geophysical data, we propose an alternative hypothesis that we shall call the 'lithospheric collision hypothesis'. In this hypothesis deformation of lithosphere on both sides of the plate boundary takes place to create the mountains. We purposefully avoid the term 'thick-skinned' (see for example, Hatcher and Hooper, 1992), because of its past usage, which includes the concept of a decollement at depth near the bottom of the crust.

Like other hypotheses, the lithospheric collision hypothesis is formulated with the observations with which the authors are familiar. Since a tectonic hypothesis is necessarily multifaceted, it must be tested by others with existing and new data from as many different subdisciplines as possible. Aspects of the hypothesis or the whole hypothesis can be falsified. A number of specific topics are suggested by these authors for further testing. Through testing, we hope to focus attention on specific problems of the Taiwan orogeny. It is with the same Popperian spirit that we tested the 'thin-skinned tectonics' hypothesis. This is especially useful in view of the multitude of relevant research being carried out or planned in and around Taiwan. By posing specific questions, we hope to make more systematic advances in our understanding of orogeny.

We shall begin by reviewing the available evidence, first geophysical and then geological, on which we base our testing and formulation of hypotheses. Then the thin-skinned tectonic hypothesis will be evaluated and lithospheric collision hypothesis proposed and discussed.

## 2. Key seismological and geophysical observations

It is probably safe to assume that before the collision began the crust under the Asian continental shelf was thinning toward the edge similar to the crust under the shelf northwest of the Okinawa Trough (Iwasaki et al., 1990) or the eastern passive margin of North America (Grow et al., 1979). Then the seismic velocity structures under Taiwan, especially any significant departures in geometry from that of a typical passive margin, can be interpreted as the results of collision-induced deformation. With the expansion and upgrading of the Taiwan seismic network in 1991 (Rau et al., 1996) the concomitant improvement in quality and increase of quantity of seismic data were significant. While more precise hypocentral locations resulted from increased station density, enhanced dynamic range of the digital recording systems broadened the magnitude range of events for which usable seismograms are recorded, and allowed the identification of more subtle first arriving phases. In addition to more detailed seismicity, tomographic imaging (Rau and Wu, 1995) using the new data now provides sufficient resolution for tectonic interpretation. With seismic velocity structures as constraints, the modeling of Bouguer anomalies of Taiwan (Yeh and Yen, 1992) is less ambiguous.

In each of the following subsections we describe the main results from relevant studies. At the end of this section we present a generalized model of the crustal and upper mantle structures under Taiwan on the basis of these results.



### *2.1. Crustal and upper mantle structures (tomography and refraction)*

Based on refraction studies using earlier local earthquake data, Rau (1992) found the crustal velocities under the Coastal Range to be similar to those of a typical oceanic crust; however, the Moho is at about 20 km below the surface. Under the Central Range, the estimate of the average Moho depth is about 38 km, and under the Western Foothills, the Moho depth is about 28 km; typical continental velocities are obtained, and the $P_n$ velocity is about 7.6 km/s.

Tomographic imaging using new data provides more details. In Fig. 2, C–C′ and D–D′ are two P wave velocity sections across the island near Hualien (see the index map in Fig. 2 for exact locations). First, a root appears to have already formed under the mountain. This root becomes noticeably shallower toward the south (Fig. 2, section B–B′ along the spine of the island). The reduction of the root (as marked by the 7.5 km/s contour) has been interpreted by Rau and Wu (1995) as a consequence of the mountain range being younger toward the south (Lee et al., 1991). Fig. 3 shows a juxtaposition of the northward-dipping Ryukyu subduction zone (from Fig. 2 section A–A′) with the velocity profile from section B–B′ in Fig. 2. This schematically shows the contact (cross-hatched area) between the Philippine Sea and Eurasian lithospheric plates. Note in section B–B′ (Fig. 2) that where the root deepens quickly the topography also rises sharply. Under the eastern flank of the Central Range, materials with velocities as high as 8.5 km/s are present at depths from 25 to 50 km (Fig. 2, sections C–C′ and D–D′); they probably represent a part of the oceanic lithosphere, and are in direct contact with the low-velocity materials on the continent side. Also seen in Fig. 2 (C–C′ and D–D′) are the relatively high velocities in the top 15 km under the Central Range, relative to velocities under the Foothills and the Coastal Plain; Rau and Wu (1995) has shown that the 5.5 km/s contours generally rise under the central Taiwan profiles to within a few kilometers under some part of the Range, although not always the highest part. Under the western Coastal Plain an extensive lower velocity (<5 km/s) surface layer is found to extend down to between 5 and 8 km. Unfortunately the resolution of tomographic inversion for southern Taiwan is very poor because of the narrowing of the Hengchun Peninsula and hence the paucity of stations in that area.

### *2.2. Seismicity, crustal rheology and focal mechanisms*

Although seismicity is an indicator of ongoing deformation, the absence of earthquakes in an area within an orogenic zone does not imply a lack of deformation, because of the dependence of rheological properties of rocks under different ambient conditions. The focal mechanisms of earthquakes allow us to map the nature of faulting, and an aggregate of them the orientation of the stresses.

#### *2.2.1. Seismicity*

The pattern of seismicity and plate configuration under and around Taiwan have been studied by Wu (1970, 1978), Cardwell et al. (1980), Tsai (1986), and Wu et al. (1989). The upgraded network has yielded much improved images of seismicity. In this paper we consider mainly the seismicity within the network, using data from 1-1991 to 5-1996; seismicity in neighboring areas can be found in earlier papers. We divide the area into three subregions: in the northern region seismicity associated with the northward-subducting Philippine Sea plate dominates; in southern Taiwan the eastward-subducting Eurasian plate is quite clear; and in central Taiwan, between these two subducting regimes, seismicity is limited mostly to the top 60 km of the lithosphere.

In Figs. 4–6 sections A–A′ through G–G′ show seismicity cross-sections in the three subregions as indicated in the index map. Although the new seismicity data do not change the basic conclusions regarding the general plate configurations around Taiwan based on earlier data, the more precise hypocentral locations define the Wadati–Benioff zones under northern Taiwan (F–F′ and G–G′ in Fig. 4) and southern Taiwan (C–C′ through G–G′ in Fig. 6) much more clearly. In contrast, the section of Taiwan between Hualien and Taitung does not have significant deep seismicity either under the island (A–A′ through G–G′ in Fig. 5) or offshore (Wu et al., 1989). In Fig. 5, seismicity permeates the upper 30–40 km in western Taiwan, with some sections (e.g., A–A′

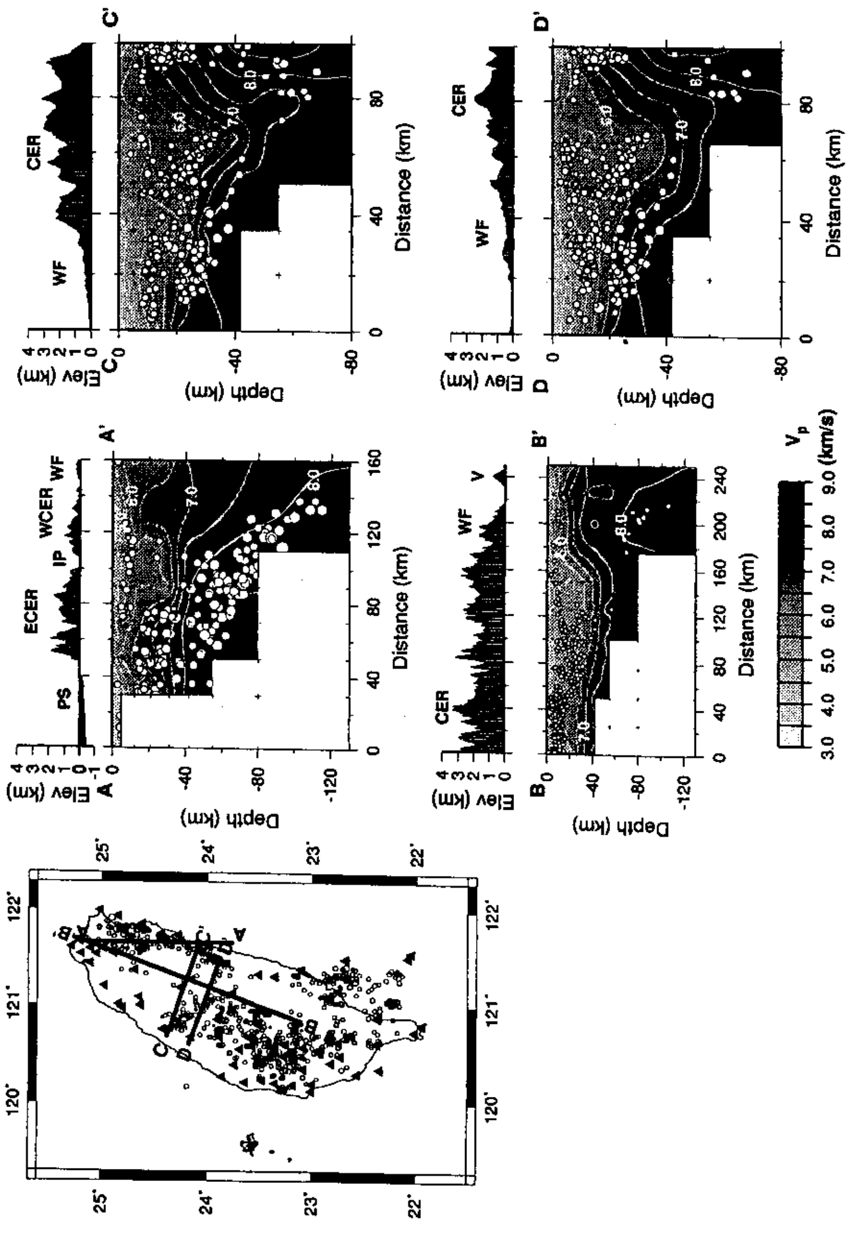


Fig. 2. Seismic P wave tomography of Rau and Wu (1995). Map shows the locations of the tomographic sections. Above each tomographic section, the topography is shown. The velocity contour interval is 0.5 km/s. The white circles are relocated hypocenters including events within ±1 grid space of the profile. The white areas mark the unsampled regions. In section *A–A'* the north-dipping subduction zone is seen clearly. It is a relatively high-velocity zone (>8 km/s) and coincides with the Benioff zone. Sections *C–C'* and *D–D'* are sections across northern-central Taiwan. Notice the presence of a root under the Central Range. Also, the seismic P velocities under the Central Range reaches 5–5.5 km/s, a velocity corresponding to relatively high-grade rocks. Section *B–B'* is along the axis of Taiwan, showing the rapid increase of the thickness of relatively low-velocity rocks (<7.5 km/s) under the northern part of the island (around the latitude of 24.5°N) and the gradual thinning from the north toward the south. *PS* = Philippine Sea; *ECER* = eastern Central Range; *IP* = Ilan Plain; *WCER* = western Central Range; *WF* = Western Foothills; *V* = Tatun volcano group; *CER* = Central Range. Note that profiles are not plotted on the same scale; in particular, B–B' is plotted at about 50% of the other profiles — the hypocenters shown in B–B' appear to be smaller in comparison with those shown in other profiles.



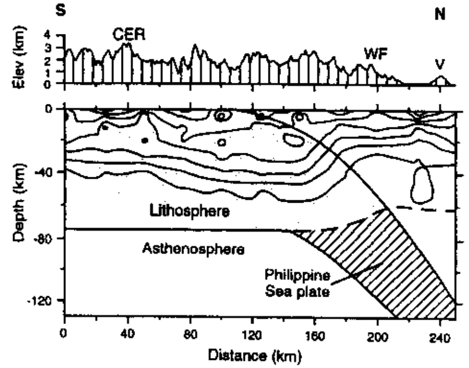


Fig. 3. Interpretation of section B–B' in Fig. 2: the thinning of the lower velocity crust can be explained as a result of younging of the collision toward the south (Rau and Wu, 1995). The collisional contact of the Philippine Sea plate with the Eurasian plate (stippled area) decreases gradually toward the north owing to the finite thickness of the lithosphere, but the two plates are in full contact south of the contact of the Ryukyu 'Trench' with the continental shelf. Note that in the B–B' section the Ryukyu subduction zone is not well developed (refer to seismicity sections B–B' in Fig. 4). The dashed line in the figure is the approximate position of the bottom of the lithosphere. Symbols are the same as those in Fig. 2.

and B–B') showing clear double seismic layers, with a zone of lower seismicity at a depth range of 15–23 km, typical of continental seismicity (Kohlstedt et al., 1995). Although double layering is not always as clearly seen in Fig. 5, curves of strain release (Benioff, 1955) as a function of depth (Fig. 7) for other cross-sections reveal such structures. Also the Central Range is generally a region of low seismicity (Wu et al., 1989), except at depth between 60 and 80 km around the 24°N latitude (Lin and Roecker, 1993; A–A' and B–B' in Fig. 5). In Fig. 4 (E–E' and F'–F') the deeper events appear to be a clump of foci just before the Benioff zone dips more sharply.

### 2.2.2. *Crustal seismicity and rheology under Taiwan*

Based on laboratory experiments on the flow law of quartz and olivine, the rheological properties of the crustal rocks under various crustal and upper mantle conditions have been derived. Kohlstedt et al. (1995) summarized the general relations among the composition, rheology, and seismicity. The curves in Fig. 8 show strength curves for two cases. At a 'normal' geotherm of 30 K/km (Fig. 8a), for example, the top part of a continental crust, down to a depth of 20 km, a friction law (Byerlee, 1978) operates, and at 20 km the quartz flow law begins to dominate and rocks tend to flow rather than behave brittly. Below the Moho, the olivine-rich rock will initially behave brittly, but soon the olivine flow law takes over and it becomes seismically quiescent. At 50 K/km (Fig. 8b), the flow law becomes effective at much shallower depth, essentially suppressing the crustal seismicity. In the oceanic crust, the olivine law rules, and the seismicity occurs throughout the crust and the upper mantle.

The observed seismicity under western Taiwan, under the Central Range and under the Coastal Range can be explained by these laws adequately as follows. The double-layer seismicity under western Taiwan discussed above represents behavior of continental crust with a normal geotherm. Under the Central Range, the geotherm is probably significantly higher as a result of two processes. On the one hand, as we have seen in the tomographic sections, the Central Range crust is formed most probably by extruding the mid- to lower crustal material; if the crust was rapidly exhumed as the fission-track data and recent geodetic data indicate (Tsao et al., 1992), the hotter lower crust would have risen rapidly, thus increasing the geothermal gradient. The second factor that may contribute to a high gradient is strain heating of the mountain (Barr and Dahlen, 1989). If the geotherm is as high as 50 K/km, much of the crustal and upper mantle seismicity can be suppressed as shown in Fig. 7b. This gradient is not unreasonable, judging from thermal gradients in wells in the Central Range (Lee and Chang, 1986). In any case, the wide occurrence of thermal hot springs in the Central Range (Chen, 1982) indicate it is an area of generally high heat flow and probably high thermal gradient. Under the Coastal Range, seismicity extends from very shallow depth down to a depth of 60 km. Two factors probably combine to achieve this. First, it is known (Rau, 1992) that the crust has a thickness of about 20 km, and that the velocities in the crust are closer to those of a typical oceanic crust than a continental one. Thus, the oceanic rheology applies here. But in order to have seismicity down to 60 km, the oceanic crust or the part of the upper mantle just below the

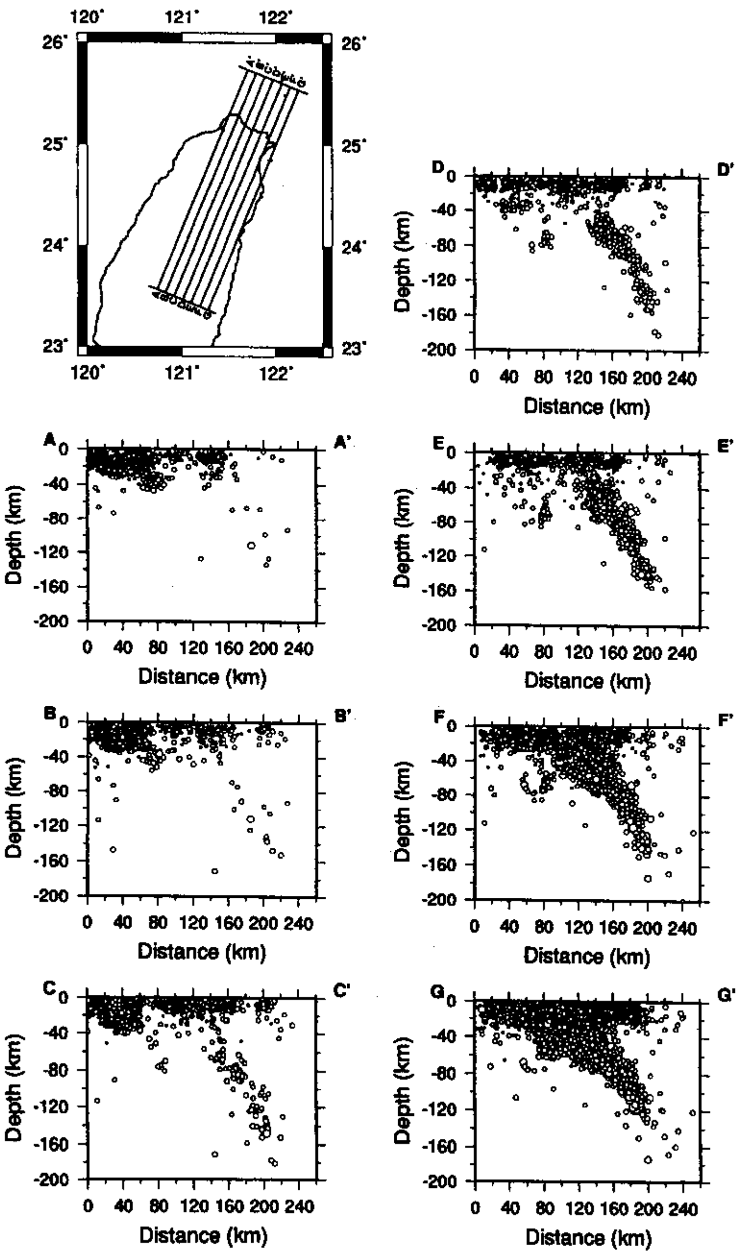




Moho probably has to be thickened, so that brittle behavior of rocks persists to greater depth. In the northern part of the Coastal Range, where the seismicity is particularly high (see Section 2.2.7 below), the focal mechanisms of moderate earthquakes do indicate some amount of westward underthrusting, and crustal thickening could occur as a result. Note that while the Central Range in central Taiwan is a relatively quiescent zone, west and southwest of Taitung, the seismicity is high throughout the crust.

### 2.2.3. *A large lower crustal earthquake*

Since the establishment of the World Wide Standard Seismograph Network (WWSSN) in 1961, only one large earthquake ($m_b = 6.2$; $M_S = 6.75$; $M_W = 6.4$) took place, on January 18, 1964, under the Western Foothills. Using WWSSN seismograms, we performed a waveform inversion employing both P and SH waves (Zwick et al., 1995) and obtained the results shown in Fig. 9a (No. 1). The estimated displacement on the fault is about 1.5 m. This earthquake evidently occurred as a blind-thrust with a relatively steep dip of 40–45° under the fold-and-thrust belt of western Taiwan.

### 2.2.4. *Normal faulting earthquake in the Taiwan Strait*

Nearly E–W-striking faults have been mapped by seismic reflection surveys in northern and southern Taiwan Strait (Chang, 1992; Lee et al., 1993). Fig. 9b (Chang, 1992) shows the normal faults mapped by multichannel seismic data in the Tainan basin. Although the Strait is also known to be seismically active (Kao and Wu, 1996), a lack of seismic stations in the area prevents detailed studies of the minor earthquakes that occurred in the area. It should be noted that a large historical earthquake of estimated magnitude 8 occurred to the west of northern Taiwan in 1604 (Lee et al., 1976).

The first instrumentally recorded earthquake in this region large enough to be studied with worldwide data occurred on September 16, 1994 (Fig. 9a, No. 2), near the western end of the Tainan basin (22.55°N, 118.74°E, depth 13 km, and $M_S = 6.5$), in the midst of mapped normal faults (Fig. 9b). Inversion of P and SH waves (Kao and Wu, 1996) shows a high-angle, dip-slip normal faulting mechanism with both nodal planes trending approximately east–west. Such a mechanism is consistent with north–south extension in the source region. The occurrence of this earthquake demonstrates clearly that the east–west striking faults in the Taiwan Strait, including those mapped by multichannel profiling, may be active.

### 2.2.5. *Anomalous shallow event in northeast Taiwan*

An earthquake took place near Nanao on June 5, 1994 (Fig. 9a, No. 3). The epicenter was located just offshore, but the aftershock locations (Fig. 9c) from the Taiwan Seismic Network showed that the fault is partially under Taiwan and trends E–W. The Centroid Moment (USGS) and the local network focal mechanisms (Central Weather Bureau, Taiwan) showed that it is dominantly a strike-slip event, and is left-lateral if it strikes E–W as suggested by the aftershock distribution (Fig. 9c). It is a shallow event at about 10 km. The WNW–ESE *T*-axis differ from those of the earthquakes farther south in the Coastal Range area, where WNW–ESE *P*-axes are usually the case. We shall explain the unusual orientation of the *T*-axis of this earthquake later.

### 2.2.6. *Internal deformation of orogen based on small to moderate* ($2.7 < M_L < 5$) *focal mechanisms*

In central and western Taiwan, the seismicity is dominated by $m_b < 4.5$ events. Through the study of focal mechanisms of minor earthquakes under the active orogen, one can get a glimpse of the mechanics of mountain building, as the earthquakes are responses to the deformation within the orogen. For small to moderate earthquakes ($2.5 < m_b < 5$), the dimensions of the corresponding faults are on the order of 10's of meters to a kilometer (Slemmons

Fig. 4. Seismicity under northern Taiwan. The seismicity included in each section is that enclosed by a box centered around the section line, with its sides half as long as the distance between the section lines. The sections in the following two figures are similarly constructed. Notice the increasingly clear definition of the Benioff zone going east from sections A–A′ to G–G′. The zone becomes continuous in section F–F′; thus the Benioff zone extends to under the Coastal Range and eastern part of the Central Range. The gradual disappearance of the Benioff zone toward the west can be clearly traced.

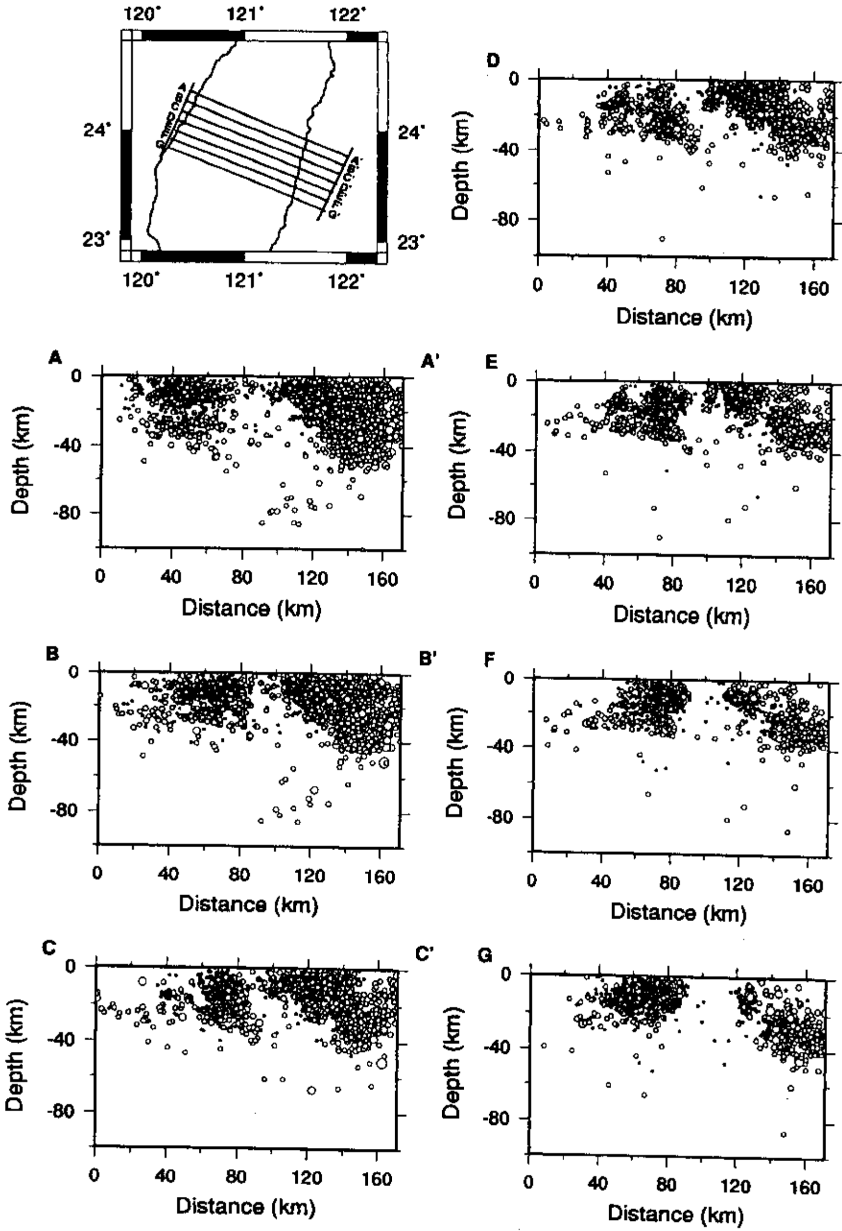


Fig. 5. Seismicity under central Taiwan. In sections A–A′ through F′–F′; a less active mid-crustal zone in western Taiwan can be discerned. The less seismically active zone under the Central Range is evident in all sections. In the eastern part of section A–A′ and B–B′ seismicity extends down to 80 km.



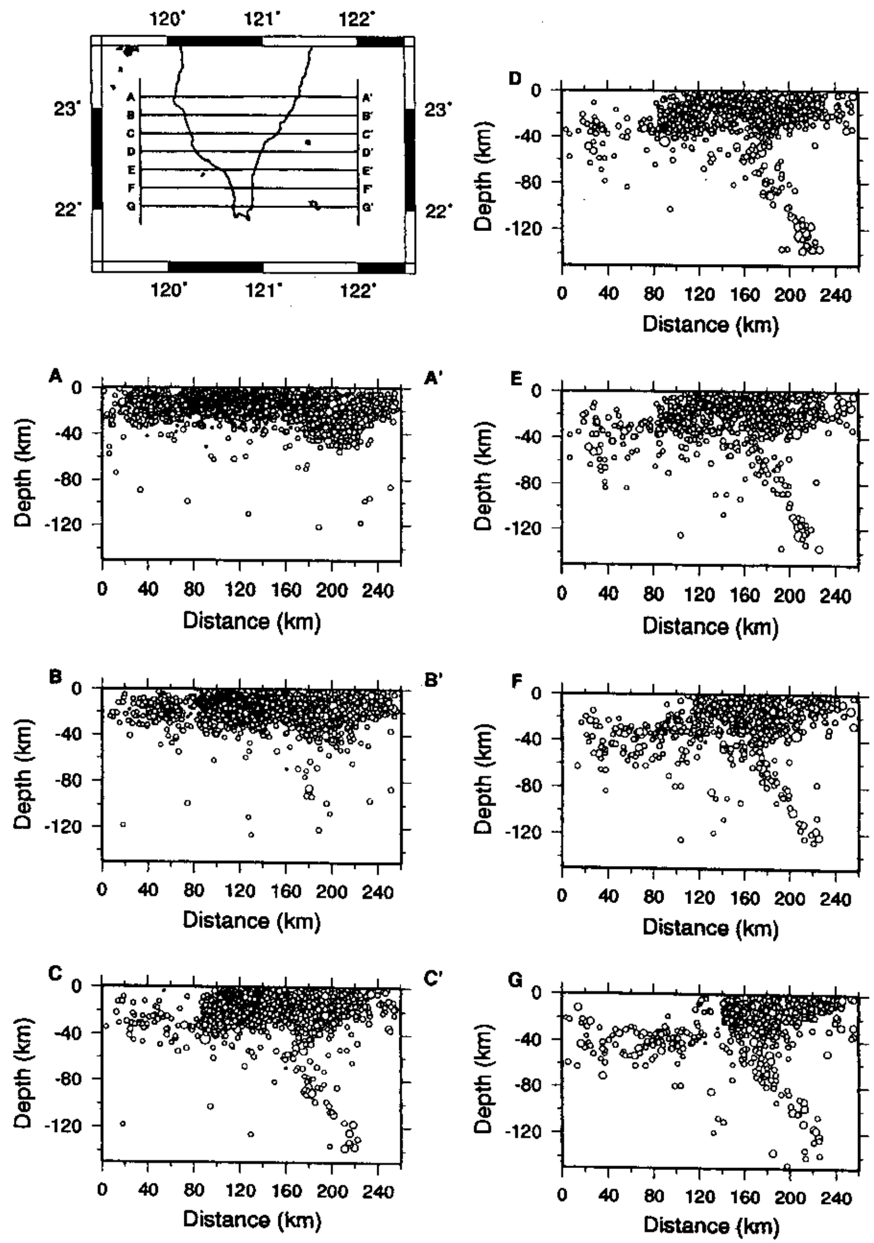


Fig. 6. Seismicity under southern Taiwan. In section C–C′ (south of Taitung) through G–G′ the east-dipping Benioff zone is well-defined. The shallow seismicity under the Hengchun ridge, the continuation of the Central Range southward, is noticeably different from the Central Range proper, i.e., no gap exists.

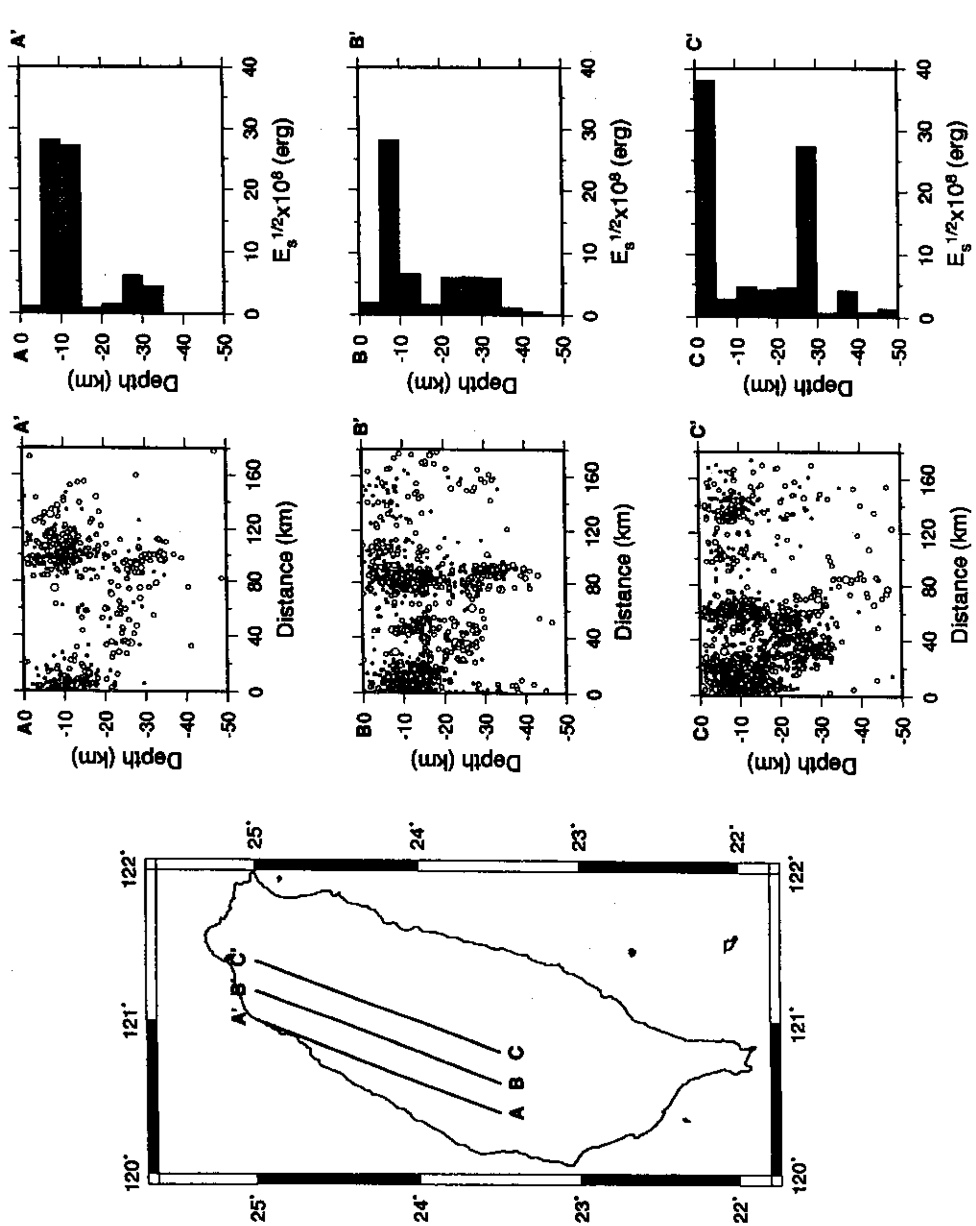

Fig. 7. Seismic double layer shown for sample sections in western Taiwan, with the locations of the sections shown on the left. From the seismicity (middle diagrams), an interval of relatively low seismicity can be seen. By looking at the energy release as a function of depth (at right), the double layering becomes clearer; energy within 5 km intervals are displayed.



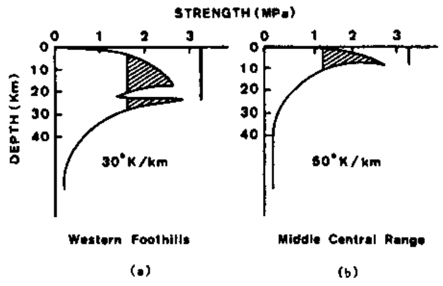


Fig. 8. Representative rheological properties of continental crust with geothermal gradients at (a) 30 K/km and (b) 50 K/km. The higher gradient is sufficient to suppress the brittle response of the lower crust below about 10 km.

and Depolo, 1986); a large number of similar mechanisms in an area probably signifies the presence of a major active structure, whereas a variety of mechanisms may indicate deformation in a highly fractured medium. Actually, the diversity of mechanism lends nicely for another purpose: the determination of local stress axes.

Using first motion polarities and SH/P amplitude ratios jointly with tomographically relocated hypocenters Rau et al. (1996) determined the focal mechanisms of 97 small earthquakes under Taiwan (Fig. 10). It is clear that mechanisms are variable even within a small region. For example, solutions 2, 6, 7, 60, and 38 are thrust faulting events at a depth range of 20–35km, and it is interesting to note that the *P*-axes are consistent, nearly horizontal and trending WNW–ESE, aligned roughly with the plate motion vector of the Philippine Sea plate (Seno et al., 1993). For another tight cluster of events at a depth range of 10–20 km (67, 82, 83, and 85–88) the mechanisms are very diverse; they are dominantly normal faulting and all of them consistent with WNW–ESE least compressive axis, instead of a WNW–ESE maximum stress axis of the last group. Three mechanism in the northern Central Range (46, 74,75) are also normal faults. That normal faulting can occur in a collision regime has been discussed extensively in a structural geologic context (Crespi et al., 1996), but the nature of faulting in situ, whether normal or otherwise, is sometimes difficult to establish. These events do indicate that normal faulting events occur in an otherwise obviously compressional regime. The occurrence of these events however, does not necessitate the occurrence of large ($M > 5.5$, say) normal faulting events, as no such events have yet occurred in the Central Range of Taiwan. In general, most of the faults are high-angle ones especially in the western Foothills, and there are a few cases where one of the planes could represent either a shallow-angle thrust (events 8, 18, and 29) or a shallow-angle normal fault (events 19, 42 59, 81, 82 and 88).

### 2.2.7. Seismicity and focal mechanism offshore of eastern Taiwan

The most active seismic area in the immediate vicinity of Taiwan is the area east of Hualien. The cross-section in Fig. 11 shows an WNW–ESE seismicity profile across Taiwan and the offshore area east of Hualien. The high level of seismicity under the Coastal Range down to 60 km and the decrease of hypocentral depths can readily be discerned. On the basis of rheological considerations described earlier, the deepening of the seismicity is interpreted as a result of the thickening of oceanic upper mantle. Although there have been a few magnitude-6 or above events in the Hualien region, there are not enough of them, especially at 30 km or deeper in the active zone, for deciphering the overall pattern of deformation. To utilize the more frequent $M_S = 5.3-6$ events Salzberg (1996) has recently implemented a combined surface and body wave inversion method. Altogether about 20 mechanisms, mostly thrusts, in this area were obtained and are shown in Fig. 11a. In depth section (Fig. 11b) they can be interpreted either as west-vergent high-angle thrusts or low-angle underthrusts. The former implies the rising of Philippine Sea materials east of the Coastal Range, and the latter provides a mechanism for thickening the Philippine Sea plate underneath the Coastal Range.

### 2.3. GPS results

Geodetic data provide direct evidence of current tectonic activity. Based on fixed and repeated mobile GPS results for the last four years, Yu and Chen (1994) presented the regional horizontal displacement (with respect to Penghu in the Taiwan Strait) and strain in the Taiwan orogen. The key findings are: (1) the volcanic island Lanhsu (Fig. 1) on the

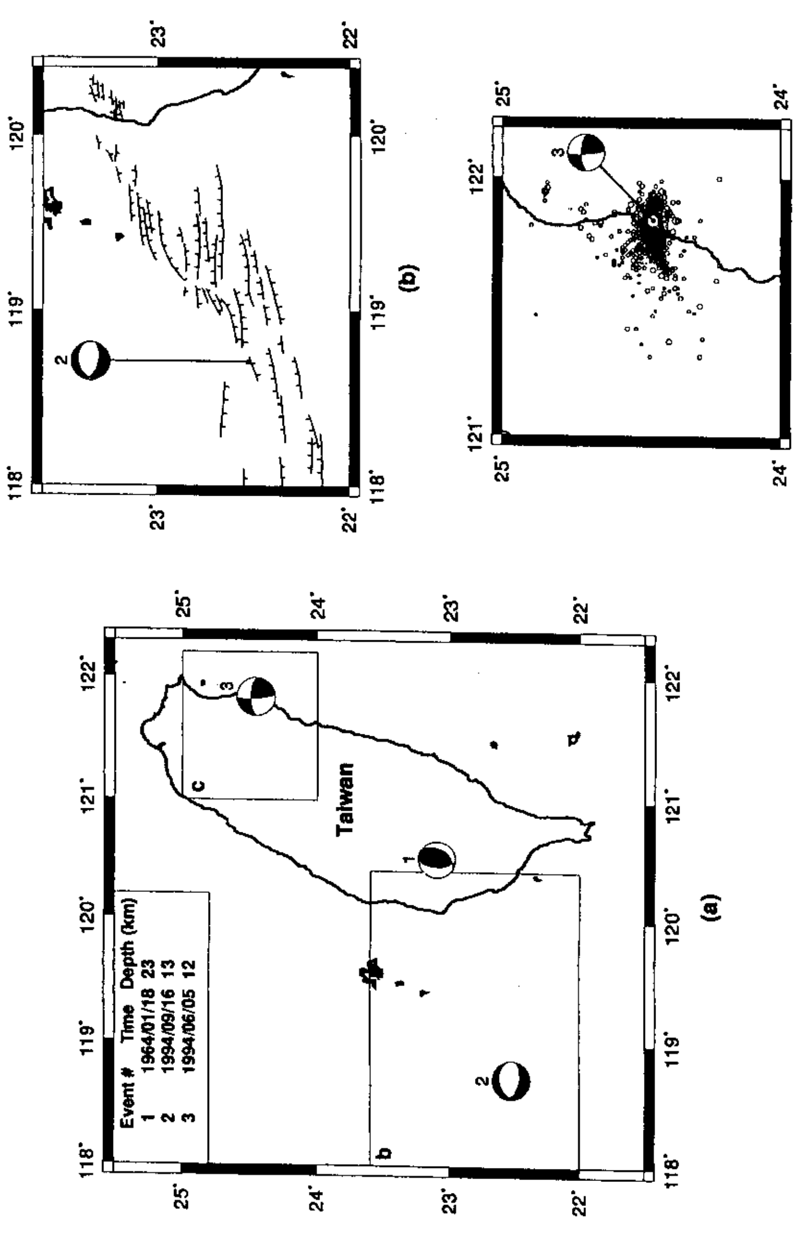


Fig. 9. (a) Focal mechanism of the three large important earthquakes in the Taiwan region; the focal mechanisms are plotted where the events are located. The focal mechanism of January 18, 1964 Tainan earthquake (*1*) derived through waveform inversion (Zwick et al., 1995). It represents a thrust fault with the centroid depth at 23 km, i.e., in the lower crust. The earthquake has a moment of $4.3 \times 10^{18}$ N m. It is located under the Foothills. The focal mechanism of the June 5, 1994 Nanao earthquake (*3*) determined by waveform inversion (USGS Preliminary Determination of Epicenters, September, 1996). The focal mechanism of the September 16, 1996 Penghu earthquake (*2*) determined by Kao and Wu (1996). (b) The location of the Penghu earthquake, its mechanism, and the normal faults mapped in the Tainan basin south of Penghu (Chang, 1992). The focal mechanism of the earthquake is consistent with the prevalent E–W-striking normal faulting in this area. (c) Distribution of aftershocks that occurred within a day of the June 5, 1994 Nanao earthquake. Its trend indicates that an E–W-striking fault plane; it is thus most probably a left-lateral strike-slip event on an E–W-trending fault, with an NW–SE *T*-axis, very different from the WNW–ESE *P*-axes of the typical thrust events south of this region (Wu et al., 1989).



Philippine Sea plate is moving at the rate of nearly 8 cm/yr toward Penghu; (2) extensional strain is found in the southern Central Range; (3) there is an overall shortening across Taiwan.

### *2.4. Bouguer anomalies*

The Bouguer anomaly of Taiwan is very conspicuous in that instead of being associated with a Bouguer low as are many older mountain ranges (e.g., Lyon-Caen and Molnar, 1983), the Central Range corresponds to a high Bouguer gradient (Yeh and Yen, 1992). The obvious low (nearly −60 mGal) in northwestern Taiwan is partially due to the thick sediments in the Taichung basin. Here we model a profile taken across central Taiwan south of Hualien (Fig. 12) where the tomographic velocity structures are well resolved. The initial density model was obtained by assigning density (Nafe and Drake, 1965) to the tomographic seismic velocities while retaining the model geometry. This 2-D density structure is then adjusted by changing slightly both the density and the boundaries until a reasonable fit to the gravity data is obtained. The boundaries in the final model have generally the same geometry as those of the initial model. From this modeling we conclude that the Bouguer anomaly profile across central Taiwan is consistent with the depression of the Moho down to a depth of 50 km and the presence of relatively high density materials at shallow depth under the Central Range. The gravitational effect of the root is balanced by the shallow high-density rocks, and the rapidly rising Bouguer anomaly in the eastern Central Range is most sensitive to the placement of the eastern flank of the root. The position of the eastern flank of the root based on gravity is offset about 7 km from that determined by tomography.

### *2.5. Summary of results*

We synthesize the above seismological and geophysical results in Fig. 13. In this figure the interpretations are superposed on 3-D plots of seismicity; the subduction zones and the major crustal and lithospheric structures are constructed based on the data presented above. We emphasize the observations that the Philippine Sea plate subducts to the north, to the northeast of Taiwan as well as under the eastern part of northern Taiwan, and the Eurasian plate subducts to the east in southern Taiwan. But from 23°N to 24°N, there is no evidence that subduction is taking place toward the east. In the figure it is also indicated that the crust under various parts of the island has thickened as a result of collision, and that the Philippine Sea plate has begun noticeably to underplate the northern Coastal Range — in what appears to be a process of lithosphere thickening. Seismicity occurs throughout much of the lithosphere under western Taiwan and under the Coastal Range. This implies that, at least, the stress is present in the crustal volume where seismicity is detected. Based on rheological consideration, the juxtaposition of the highly seismic region under the Coastal Range, down to a depth of 60 km or more, against the seismically quiescent Central Range evidently reflects the transition from oceanic crust to continental crust. The southern tip of Taiwan, overlying a well-defined Benioff zone, is an accretionary wedge, with relatively thin crust.

## 3. Tectonic geology of Taiwan

### *3.1. Geologic framework of the island of Taiwan*

The part of Taiwan west of the Longitudinal Valley (Fig. 1b) was in a passive continental margin and slope environment before the impingement of the Luzon Arc that created Taiwan (Chai, 1972). The dominant geologic variations resulting both from the orogeny and the orientation of the sedimentary basin occur in the direction perpendicular to the trend of the island, with rocks generally becoming older, more metamorphosed, and more intensely deformed when proceeding eastward. The western Taiwan Foothills (Fig. 1b) are composed of Plio–Pleistocene rocks in a fold-and-thrust belt (Ho, 1988). The source sediments of these rocks are from the Central Ranges, i.e., they are post-orogenic. To the west of the Foothills is the Coastal Plain, where recent sediments are rapidly accumulating. In the Central Ranges east of the Foothills, the older Tertiary (Paleogene) shelf and slope sediments are metamorphosed to become mostly slates and schists and are now raised to a maximum elevation of nearly 4000 m. But higher-grade metamorphic rocks of pre-Tertiary age are exposed on the eastern flank of the Range. These rocks had been subjected to

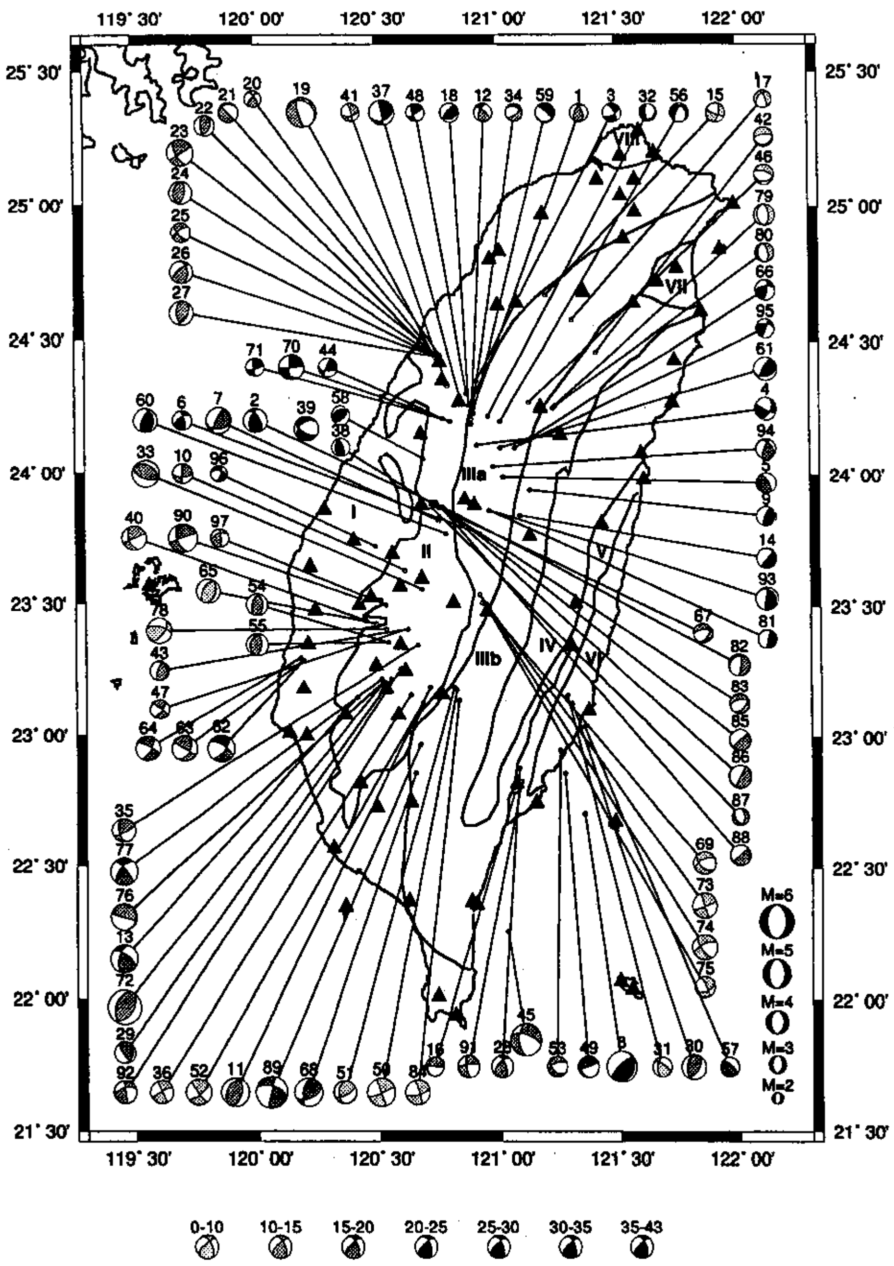




deep burial (>10 km) and represent those of mid-crustal level. East of the high-grade metamorphics is the Longitudinal Valley, a sediment-filled, relatively linear valley separating the Central Range from the Coastal Range in eastern Taiwan. The Coastal Range is composed of a suite of rocks that were associated with the island arc on the margin of the Philippine plate. It is capped by andesites of the Luzon Arc, with the underlying sedimentary rocks consisting of deposits in the forearc basin, in the trench and on the outer rise. Considering the distance between the volcanic arc and the trench, shortening of more than 100 km of the Philippine Sea plate margin must have been accommodated.

The north–south geologic variations in Taiwan are more subtle. For example, the Central Range can be divided into the Hsueshan (in the west) and the Backbone (in the east) ranges in northern Taiwan; the Paleogene rocks in the Hsueshan Range are coal-bearing and were deposited in a typical continental shelf environment, while the rocks in the Backbone Range are finer grained and were deposited close to the continental slope. Between 22.8°N and, 23.5°N, however, only the equivalent Backbone Range is there. In other words, at that point, the orogen is moving off the shelf and onto the slope.

No detailed geologic map of southern Taiwan, south of the line connecting Kaoshiung and Taitung, has yet been published, although the mélange at the southern tip of Taiwan has been a focus of attention (Ho, 1988). Generally the slates in the southern Central Range north of this area grade into unmetamorphosed rocks of the Hengchun Peninsula. Hu and Tsan (1984) mapped the structures along the southern Taiwan railroad and found them to be quite different from those of the Central Range further north. In addition to the dominant N–S-striking folds, they also mapped a number of small-scale E–W striking folds and right-lateral strike-slip faults. They concluded that after the compression under ENE-oriented stress in the Plio–Pleistocene, there had been N–S-oriented compression operating in this area. These observations point out that the area is in a tectonically very different environment from that of the Central Range.

### 3.2. *Accretionary wedge onshore and offshore of southern Taiwan*

Reed et al. (1992) mapped the offshore area of southern Taiwan, defined the accretionary wedge, and show the geometry of the wedge as well as the ubiquitous thrust faulting therein. Several investigators (e.g., Lee et al., 1993; Gong et al., 1995; Lallemand et al., 1995) have attempted to trace the northern terminus of the deformation front. While Lee et al. (1993) and Gong et al. (1995) connect it to structures on shore near Kaoshiung, Lallemand et al. (1995) prefer a more northerly location. Lee et al. (1995) used multichannel seismic data to show the continuity of the deformation front as mapped by Reed et al. (1992) to Kaoshiung and the absence of any displacement in the channel deposits west of Tainan in the Strait. At present the Kaoshiung connection seems to be better supported; Kaoshiung is also the point south of which the east-dipping northern Luzon subduction zone becomes clear (Fig. 6, C–C'). The southern part of Taiwan and offshore of southern Taiwan clearly belong to the accretionary wedge environment.

The deeper crustal structures are being studied with the 1995 R/V *Ewing* multichannel data (Don Reed, pers. commun., 1996) and wide-angle sea–land reflections (Yeh et al., 1995). From the Bouguer anomalies (Fig. 10) in southern Taiwan we can see the transition from the generally negative Bouguer values northwest of Taitung to positive values southwest of Taitung; it is quite possible that the Hengchun Peninsula is underlain by mostly oceanic crust. This is particularly an important problem in understanding how the Hengchun ridge was formed.

Fig. 10. Map of Taiwan showing the locations and fault plane solutions of 97 events studied (Rau et al., 1996). The solutions are coded for both local magnitude (2–6) and depth (0–43 km). The numbers next to the solutions indicate time sequence, the later the event the higher the number. Seventy-five TaiSeiN seismic stations are shown as solid triangles. The solid lines mark the boundaries of the major geologic units: *I* = Coastal Plain, *II* = the Western Foothills, *III* = the western Central Range, *IV* = the eastern Central Range, *V* = the Longitudinal Valley, *VI* = the Coastal Range, *VII* = the Tatun volcanic group.

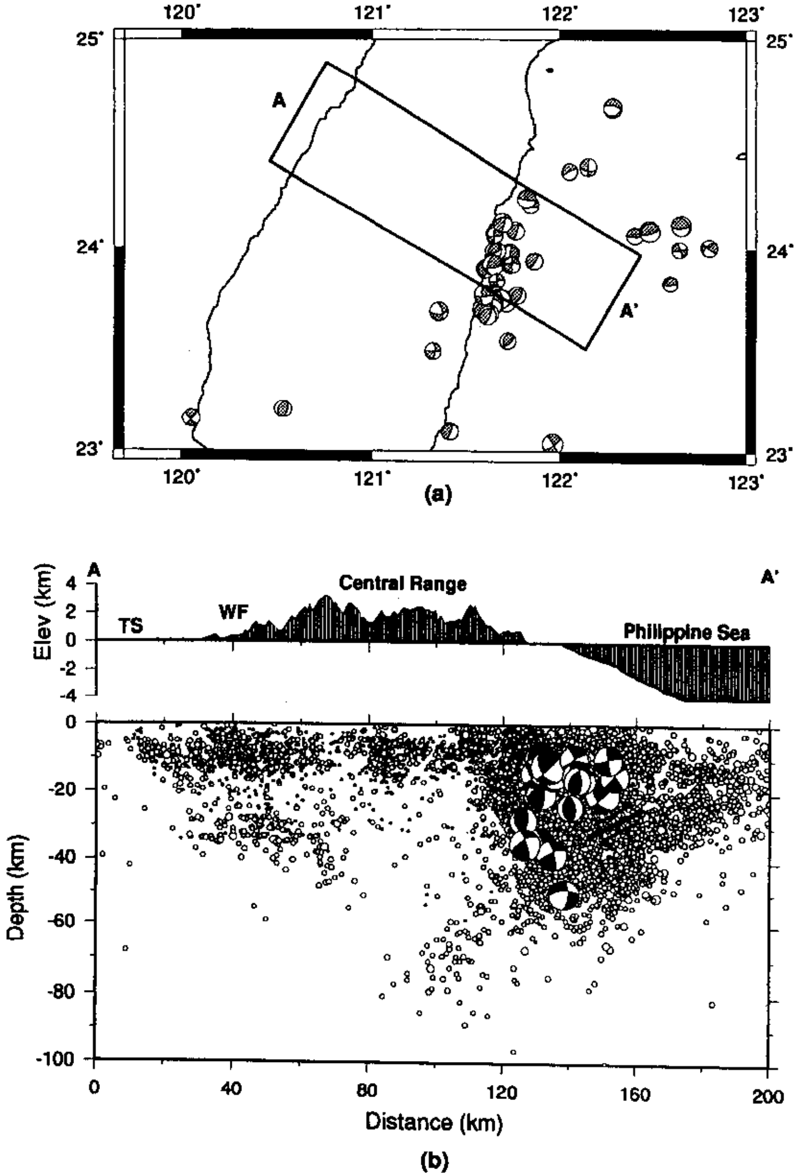


Fig. 11. (a) Focal mechanisms of $5 < M_S < 6$ events near Hualien. (b) A NWN–ESE seismicity profile across Taiwan contained in the box shown in (a) and the focal mechanism of the same events as in (a), but shown in the vertical plane parallel to the section. There is an apparent shallowing of foci toward the east, under the Philippine Sea; note that because only land-based data are used, the depth determination of offshore earthquakes may have errors up to 30 km.



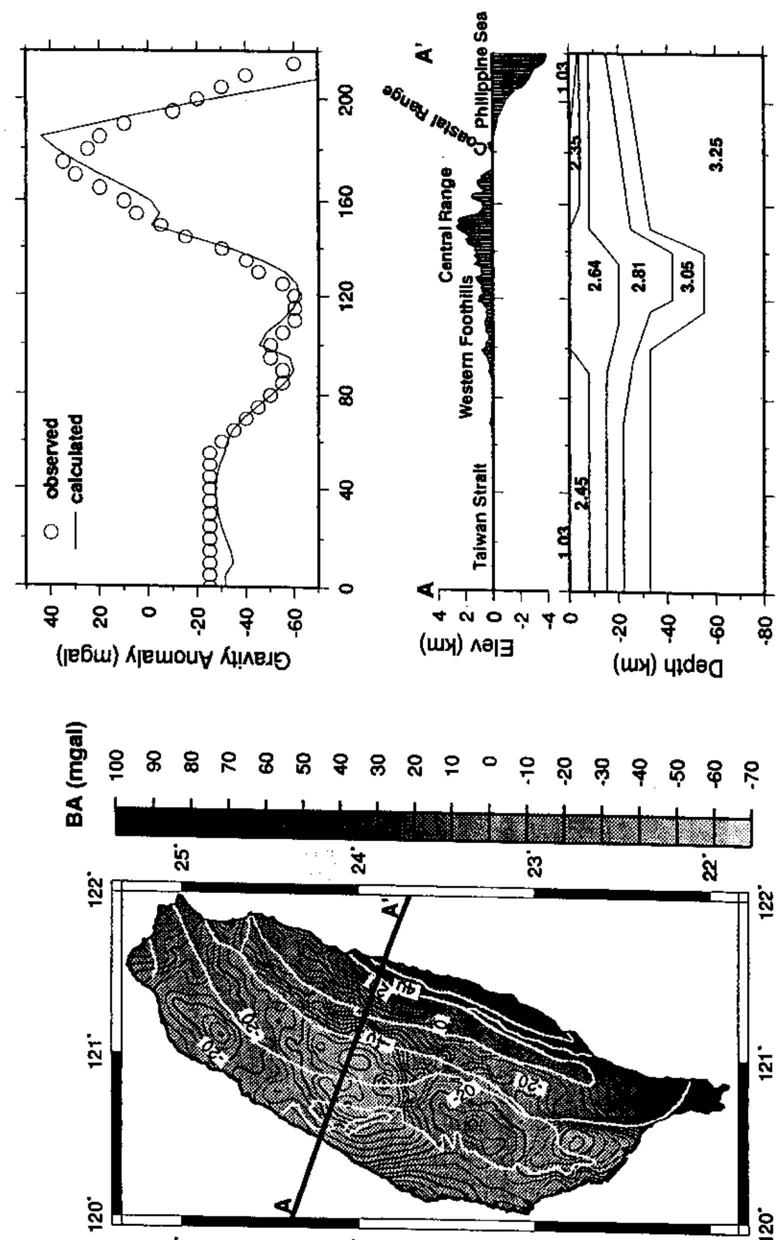


Fig. 12. 2-D Bouguer gravity interpretation constrained by a tomographic seismic velocity model. The distances between 70 and 170 km in A–A′ correspond to the D–D′ profile in Fig. 2. For lack of constraints the gravity anomalies offshore are not well modeled.

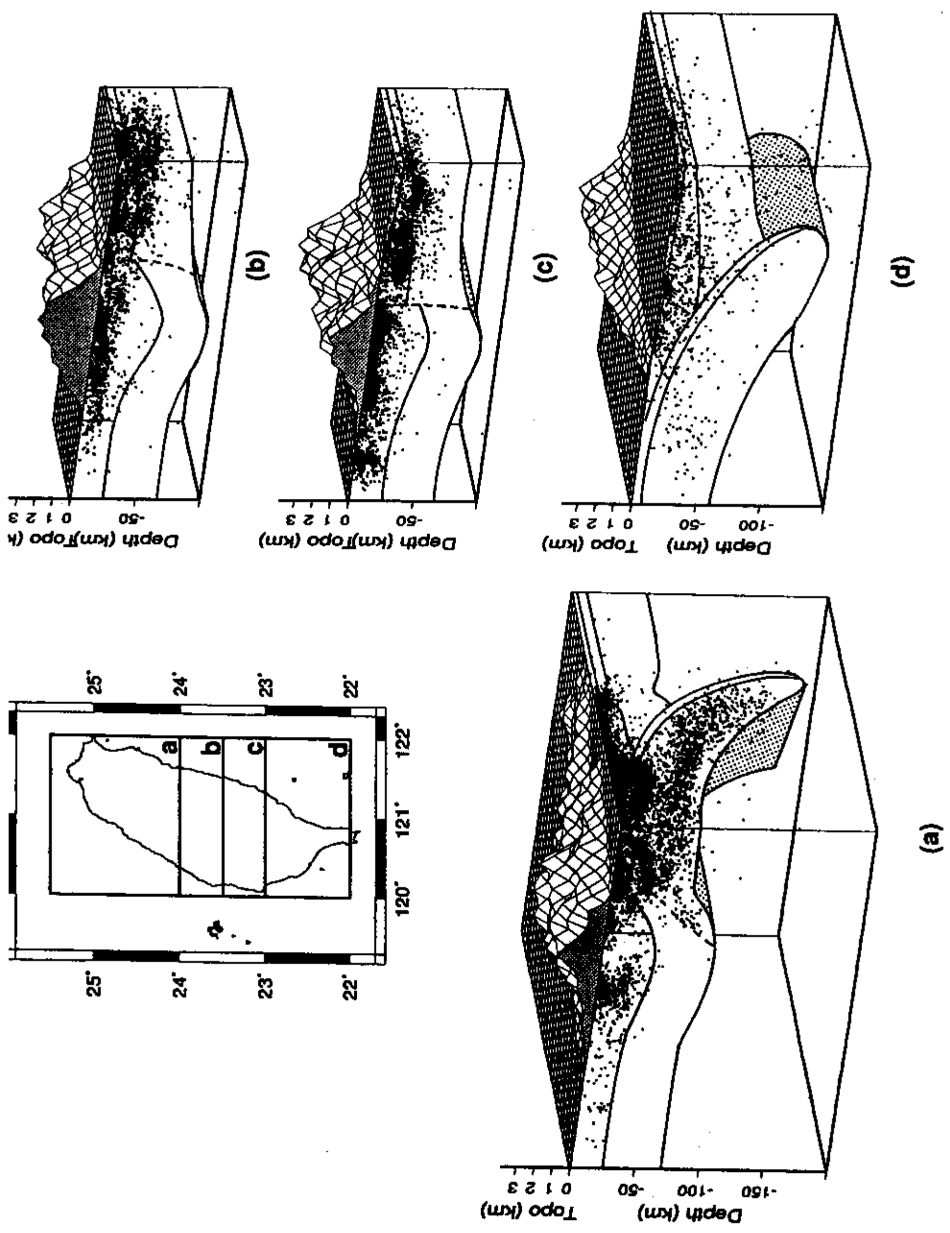


Fig. 13. Synthesis of seismological and geophysical data showing major subsurface structures. The structures are superposed on the 3-D seismic foci. The depth of the crustal features are those from seismic tomography (Fig. 2). The WNW motion of the Philippine Sea plate led to both northward subduction of the Philippine Sea plate (a) and the collision of the lithospheres of this plate and that of the Eurasian plate, resulting in the thickening of the crust and the lithospheres on both sides (b and c). In southern Taiwan, the Eurasian plate subducts eastward under the Philippine Sea plate (d). The locations of the blocks are shown in the index.



Since the deformation front west of Hengchun is not yet in contact with the Eurasian continental shelf, the Hengchun Peninsula and the ridge south of it could not have been created through collision in the same manner as the Central Range.

### 3.3. Geology offshore of eastern Taiwan

The area offshore of the east coast of Taiwan (between 23°N and 24.5°N and from the east coast to 123°E) is tectonically complex. A number of shallow penetration, multichannel and single-channel seismic lines have been gathered by National Taiwan University and they have been summarized and interpreted by Lin (1994). Here the deformation associated with the Ryukyu forearc and that of the collision of the Philippine Sea and Eurasian plates are evidently superposed. The Yayaema ridge (Fig. 14) is the southwest continuation of the Ryukyu forearc and appears to be a fairly typical accretionary wedge overlying the subducting Philippine Sea plate as shown in Lin's seismic sections. In approaching the Coastal Range of Taiwan, the EW-striking forearc appears to be truncated by island-parallel ridges and troughs. Southeast of the intersection of Ryukyu and Taiwan is the Hoping Basin, east of the precipitous cliff between Hualien and Nanao. This is a very curious basin as it is apparently quite deep and associated with a remarkable free-air gravity low of about −200 mGal (Yen et al., 1995). Wu (1978) interpreted this basin as having been created under E–W tension. The orientation of the *T*-axis of the June 5, 1995 earthquake described above is consistent with this interpretation. South of the Ryukyu Trench on the abyssal plain, the sedimentary layers are generally undisturbed, although several large strike-slip seismic events were located there (Wu, 1978).

### 3.4. Falsification of hypothesis

In terms of orogeny, a truly comprehensive hypothesis should include the space–time evolution of a

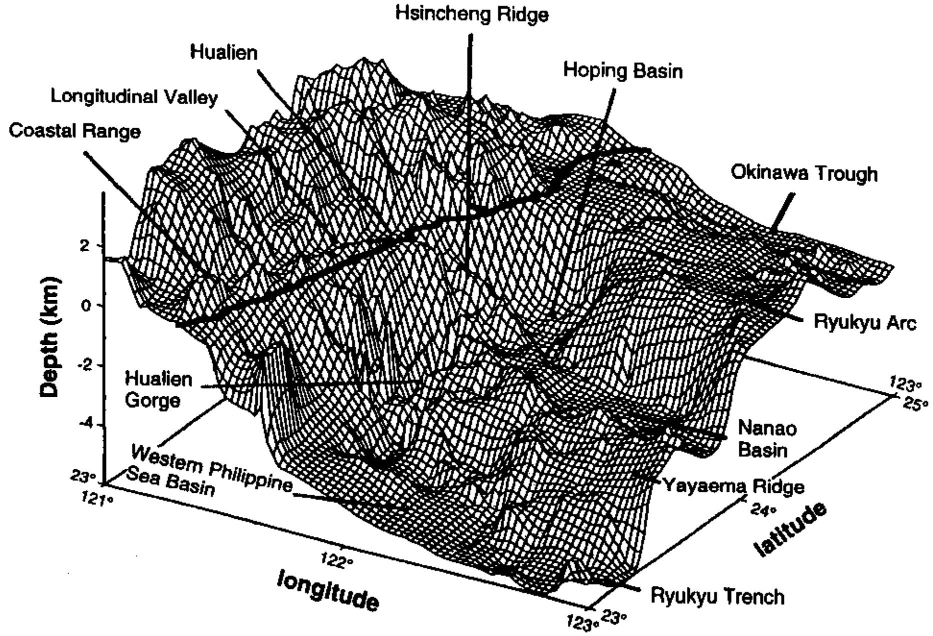


Fig. 14. 3-D view of the bathymetry offshore of northeastern Taiwan (adapted from Lin, 1994).

mountain range. Even for the young Taiwan orogeny, such a hypothesis does not seem to be within grasp yet. In the meantime, a hypothesis may center on the evolution of a mountain belt, for which dating of events are needed. The hypotheses we attempt to falsify and propose concern mainly the orogenic processes that led to the current state. The observables are the results of the processes: the geometry of boundaries and the nature of materials as interpreted from seismicity, velocity and density. Through the focal mechanisms and GPS measurements we can also map the current state of strain. Although the three dimensions of the physical space may be well sampled, the data are time-insensitive.

In this paper we follow the view of Popper (1968) that a scientific hypothesis cannot be shown to be absolutely true, and it should be subjected to constant falsification attempts. We shall use existing data as summarized above to test the thin-skinned hypothesis of Taiwan orogeny, and finding it inadequate we then offer a new hypothesis. The new hypothesis should then be subjected to tests by others. We make attempts to show what are the unsubstantiated assumptions of our hypothesis to facilitate testing. We believe that through such a process, attention can be focused on key questions of the Taiwan orogeny.

## 4. The thin-skinned tectonics hypothesis of the Taiwan orogeny

### 4.1. The thin-skinned model

Suppe (1981, 1987) pioneered the modeling of the Taiwan orogeny in terms of 'thin-skinned' tectonics. His interpretation arose primarily from mapping of the fold-and-thrust belt in western Taiwan (Suppe, 1976), and was later augmented with exploration seismics and some drilling data in western Taiwan (Suppe, 1980, 1981). Davis et al. (1983) explicitly made the fold-and-thrust belt and the accretionary wedge equivalent and Dahlen and Barr (1989) then solved the thermal–mechanical problem of a 'critical' wedge. This model is based on the following assumptions: (1) the boundary between the Eurasian and the Philippine Sea plates extends from the Manila Trench northward onto the Coastal Plain of western Taiwan, and the east-dipping subduction zone in northern Luzon also continues northward with the continental lithosphere under Taiwan subducting to the east; (2) the Taiwan orogen is wedge-shaped and is soled by a decollement, at a slope of about 6°, which coincides with the top surface of the subducting plate; and (3) the materials in the wedge follow a cohesionless friction law under supra-lithostatic fluid pressure.

More specifically (Suppe, 1987), the Tertiary sediments in Taiwan that dominate the surface geology of the mountain ranges fill the wedge; they are folded and faulted in a brittle manner above a detachment (Fig. 15A, B) such that they can be retrodeformably reconstructed. A 'bull-dozer' or indentor, the Coastal Range, came from the east and deformed the wedges on the continental shelf and the Philippine Sea plate to form the mountain range (Fig. 15C). New materials enter the wedge from the west and are moved closer to the indentor along paths that are depth-dependent; they, however, will be exhumed. The metamorphism of the materials intensifies as they move through the wedge. The rate of propagation of the apex of the wedge is assumed to be constant, and is the same as the indentor. Erosion continues to remove materials from the surface of the wedge. With the erosion rate and the rate of uplift assumed to be nearly in balance, the wedge maintains a steady-state cross-section. The wedge, at its deepest point is on the order of 10–20 km. This model is essentially two-dimensional in the sense that the geological differences along the axis of Taiwan are considered to be only a result of southward propagation of the collision.

### 4.2. Falsification of thin-skinned model and discussion

Whereas the thin-skinned hypothesis predicts that the Taiwan orogeny is a result of the deformation of an accretionary wedge-like body with depth not reaching beyond about 20 km, the observations outlined above indicate that the orogeny in Taiwan involved the deformation of the whole crust and upper mantle. Instead of being limited to a shallow wedge, a root as deep as 50 km under the Central Range, a result of long-term deformation, had formed. Major deformation that must be associated with the ongoing orogeny is also occurring beneath the assumed wedge. There is no evidence supporting the subduc-



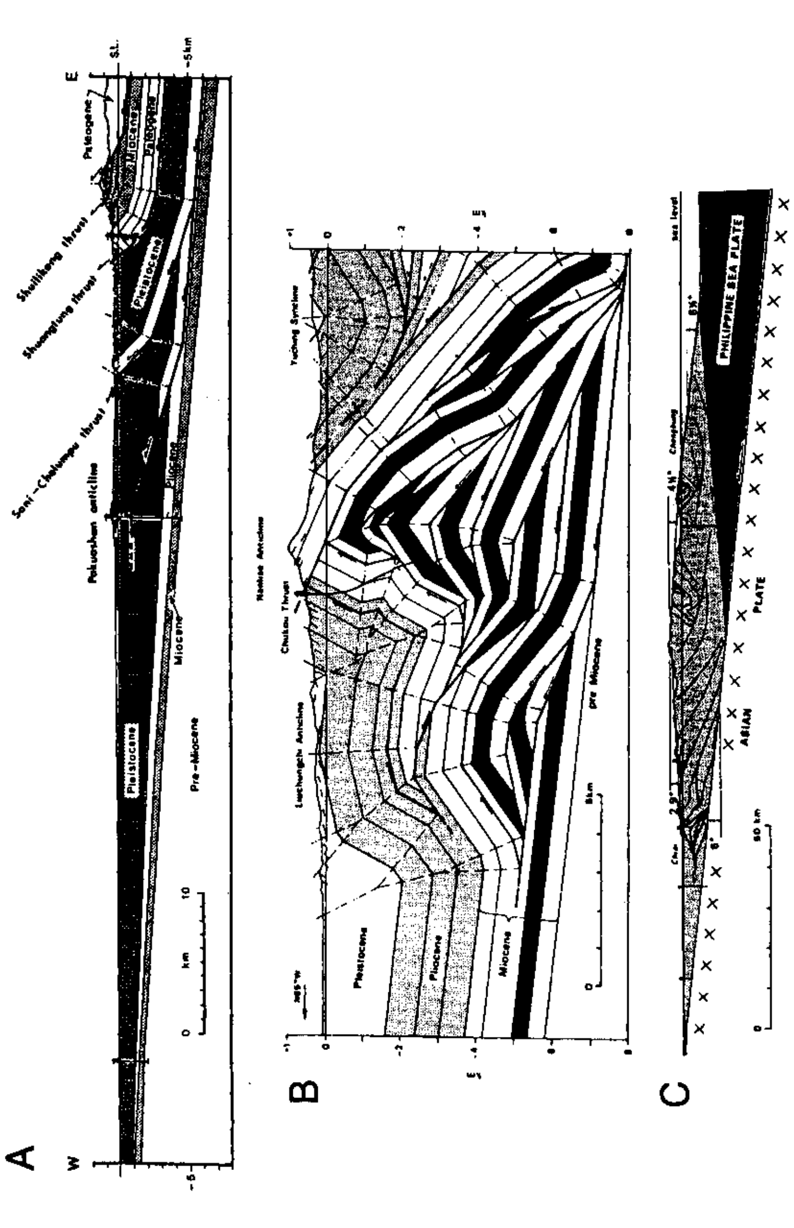

Fig. 15. (A, B) Thin-skinned tectonics of Taiwan as illustrated by a cross-section across central Taiwan (Suppe, 1987). Here a decollement underlies the Miocene sediments (shown as folded and faulted layers). (C) In this model the Central Range is created by advancing the Philippine Sea plate westward.

tion of the continental lithosphere under the Central Range, whether in terms of a dipping seismic zone, normal faulting on the outer rise (with *T*-axis perpendicular to the trend of the island), or shallow thrust events under the Foothills. Also, with seismic velocity around 5.5 km/s, the rocks at shallow depth under the Central Range are most probably metamorphic rocks similar to those exposed on the eastern side of the Central Range and not likely to be in a critical state. The Taiwan orogeny as a whole also is closely coupled to the lithospheric shortening at the margin of the Philippine Sea plate near Taiwan as well as the faulting in the Taiwan Strait. Thus the thin-skinned tectonics is not adequate or appropriate as a hypothesis for the Taiwan orogeny.

We falsify the thin-skinned hypothesis based mainly on the observations that the Central Range is not modeled correctly and important orogenic processes at depth are not included. However, there are questions concerning the fold-and-thrust belt in the Foothills that we did not address. For example, the existence of a decollement as a base for such a belt is frequently invoked in orogenic studies. Neither in the seismicity or small earthquake focal mechanisms obtained so far can a decollement be discerned. In the 'thick-skinned' tectonics of Hatcher and Hooper (1992) a decollement is defined more loosely as a zone of mechanical weakness along which faults may propagate. They propose that the decollement may exist near the transition between the brittle and ductile layers or in the ductile layer in the crust. Of course such a decollement would play a very different role from the one assigned in the thin-skinned hypothesis. There are other related aspects of the falsification, but we shall avoid repetition by discussing them later after we describe the proposed lithospheric collision model.

### 4.3. The lithospheric plate collision model

In this hypothesis the Taiwan orogeny is the result of a collision between the Eurasian and the Philippine plates with the plate edges engaged in collisional (transpressional) contact. Since the Philippine Sea plate is subducting toward the north at the same time, the contact area between the two plates is variable as shown in Fig. 3. The two plates are in contact from the surface down to a depth of more than 60 km near Taitung (23°N), but as the Philippine Sea plate begins to subduct northward near 23.5°N the top of the contact zone begins to dip northward; initially the dip is small, but it increases gradually and north of Nanao the subducting Philippine Sea plate dips under the lithosphere and encounters the asthenosphere on the Eurasian side (Fig. 3). Beyond the northern tip of Taiwan, the two plates are no longer in collision. Due to the non-parallel orientations of the Luzon Arc and the Eurasian continental shelf, the contact was first established near Hualien and moved south, toward Taitung, as a function of time; south of Taitung, collision has not yet begun as the Eurasian continental shelf has turned more sharply westward. On the continental side, the creation of the Central Range involved the thickening of the crust as well as the upward extrusion of the mid- and lower crustal materials (Fig. 16a). The fold-and-thrust belt in the Foothills region is formed by stresses transmitted across the Central Range and the deformation extends down to below the Moho. While the deformation under the Central Range is dominated by

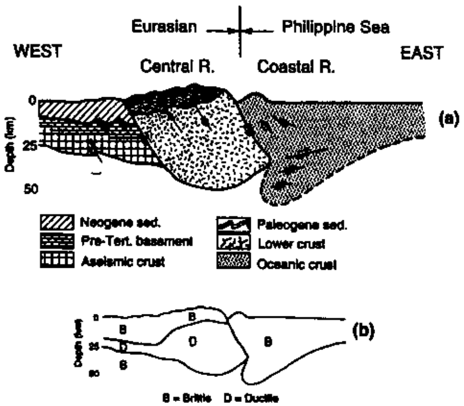


Fig. 16. (a) Schematic cross-section of the proposed lithospheric model. In this model the lithospheres (approximately 100 km thick) of the Philippine Sea plate and the Eurasian plate are engaged in collision, without subduction of either plates. The collision has resulted in the thickening of the crust, through downwarping as well as the extrusion of the mid- and lower crust, whereby the Central Range was uplifted. Note that the whole lithosphere probably has been deformed in the orogeny as indicated in Fig. 13. (b) Schematic rheological composition of the Taiwan orogen as suggested by distribution of seismic foci.



flow, the crust and upper mantle form a sandwich of strong–weak–strong–weak materials that deform by brittle deformation in the strong layer and flow in the weak layer (Fig. 16b). On the Philippine Sea plate side, thickening of the crust has accompanied shortening which has resulted in the stacking of the volcanic arc, the forearc and the trench sediments in the Coastal Range. The area west of Taiwan is dominated by N–S tension resulting from transmission of stress in the brittle layer on top or from flow in the ductile layer. A representative cross-section of the model is shown in Fig. 16, the overall plate interaction and the 3-D features are illustrated in Fig. 13.

### 4.4. Discussions of the model

The hypothesis described above is very general. The agreement with available observations described earlier can be easily established. There are many implications however that are candidates for use in falsification. We shall discuss some of the details and deductions of the hypothesis as we see it.

The oblique (N70°W) convergence between the Philippine Sea and the Eurasian plates partitions into the shortening of the margins of both plates and northward (actually NNE) subduction. The suture between these plates can be discerned in the tomographic images (Rau and Wu, 1995), and from differences in seismicity as described earlier. The convergence thickened the whole crust to form a root under the Central Range and also raised the mid- to lower crust to shallow depth to build the Range; the relatively high-velocity (5.5 km/s) and high-density rocks are probably similar to those in the Pre-Tertiary eastern Central Range. At the same time, both the crust and the upper mantle of the Philippine Sea plate margin have been thickened to build the Coastal Range. The Tertiary strata in the Central Range are not more than a few kilometers thick and lie directly on the Pre-Tertiary basement rocks similar to those now exposed on the eastern side of the Central Range. The Western Foothills are underlain by a thick sedimentary basin filled with post-Late Pliocene rocks that were shed from the Central Range. These rocks are deformed as a fold-and-thrust belt by stresses transmitted across the Central Range; folding and blind-thrust faulting occur within the brittle layers in the upper 40 km of the crust. The lithosphere is a sandwich of brittle–viscous–brittle–viscous (upper crust–lower crust–upper mantle) layers. The collisional effects are also transmitted to the western Taiwan Coastal Plain and to Taiwan Strait; E–W oblique right-lateral strike-slip/normal faults occurred in association with several earthquakes within this century and E–W-striking normal faulting in the Strait.

Based on both seismicity (Fig. 4) and tomographic imaging (Fig. 2, A–A′ and Fig. 3), it is evident that the intersection of the westward extension of the Ryukyu Trench and the Taiwan orogen is located south of Hualien. The exact location is probably not as important, as the slope of the subduction zone is initially very small. The subduction zone actually appears to underplate the eastern part of Taiwan south of Hualien. The changing geometry of the collisional contact should affect the variation of intensity of the orogeny as well as the style of deformation along the Central Range. Between Hualien and Taitung the two sides of the plate should essentially bear the full brunt of the collision and therefore this section should undergo the largest shortening. Further north, the Philippine Sea plate is impinging on the lower part of the Eurasian lithosphere. Between Hualien and Nanao, the compressional contact is placed at increasingly greater depth toward the north; the overall shortening on the Eurasian side is still expected to take place. The Eurasian plate above the Ryukyu subduction zone to the east is decoupled from the subducting Philippine Sea plate and will not be compressed. As a result, we can expect the separation of the Eurasian plate along the Hualien–Nanao line. Here WNW-trending tension is generated. That such a stress condition exists may be shown by normal faulting in the Hoping basin (Lin, 1994). The WNW–ESE-oriented tension such separation would generate is also consistent with the focal mechanism of the June 5, 1994 earthquake cited earlier.

The oblique collision of the Luzon Arc with the Eurasian margin implies a shift of the point of contact southward with time (Suppe, 1984). A rate of 90 km/m.y. was estimated by Suppe (1984) adopting the trend of Taiwan as the orientation of the Luzon Arc before collision and taking the line connecting the shelf south of Penghu to the middle of the Okinawa Trough near northeastern Taiwan as the edge of the shelf before collision. Lee et al. (1991) used the block rotation in the Coastal Range as a proxy for determining the time of contact of the Luzon Arc with the shelf and their rate is 40 km/m.y.; the contact near Hualien occurred about 3.5 m.y. ago and reached Taitung about 1 m.y. ago. This is much slower than Suppe's estimate. The two rates can be reconciled if, using Suppe's geometric construction, the trend of the present Luzon Arc (N10°W) is taken as the trend of Luzon before collision and if the shelf line is constructed by linking the shelf south of Penghu to the southern edge of the Okinawa Trough, i.e., assume that the back-arc spreading was not as extensive as previously estimated. Suppe (1984) further assumed that the propagation began in northernmost Taiwan and has now reached the southern tip of Taiwan. Part of the reason for extending the propagation to northern Taiwan is to account for the orogeny northwest of Hualien. Our hypothesis has obviated this view by invoking the finite thickness of the lithosphere, whereby the orogeny persists north of Hualien as the Philippine Sea plate continues its northward subduction as well as its collision with the Eurasian plate.

As far as the southern extent of the collision is concerned, we have seen that south of the Kaoshiung–Taitung line, the southern part of Taiwan can be described as a true accretionary wedge overlying a subduction zone, while north of this line the collision involves the deformation of the continental crust. Thus there must be a discontinuity or, more likely, a transition zone in the vicinity of this line; in the south, the materials between the volcanic arc and the deformation front is undergoing shortening while the deformation front continues to move westward to approach the Eurasian continental shelf and in the north, the orogeny described above is taking place (Wu, 1996). The transition is partly a left-lateral fault and partly the result of a southward extrusion, or escape, of the Central Range. It is possible that the GPS results in southern Taiwan (Yu and Chen, 1994) are showing that the Hengchun Peninsula is moving westward relatively to the Coastal Plain north of Kaoshiung. Recall that the Coastal Range of eastern Taiwan is actually a telescoped suite of island arc volcanics, an accretionary wedge and trench sediments, an equivalent coastal range to the west of the Hengchun Peninsula may be formed in about six million years on the continental shelf of SE China, incorporating the Lutao–Lanhsu volcanic arc, the Hengchun Peninsula and the sediments to the west of Hengchun.

The normal faulting in the Taiwan Strait is a problem of far-reaching consequence. The problem of producing normal faulting in an otherwise compressional environment has been explored (Burchfiel and Royden, 1985; Burchfiel et al., 1992; England and Molnar, 1993). In the Taiwan Strait, the strike of the fault is nearly parallel to $\sigma_1$, the maximum principal compressive stress, similar to the normal faulting on the Tibetan Plateau, north of the Himalayas. But in this case, neither collapse of a high plateau or a cessation of collision, causes invoked by England and Molnar (1993) applies. Kao and Wu (1996) proposed the following two alternatives. Analogous to the model that Zhao and Morgan (1987) proposed to explain the rising of the Tibetan Plateau, we propose that flows may be generated in the ductile layers in the lower crust and upper mantle (the aseismic layer in the lower crust or the aseismic layer in the mantle). While the flow in the lower crust may be linked to the ductile flow in the Central Range, the upper mantle flow results from the push by the Philippine Sea plate and the root formation. When either flow diverges to the north and south, local N–S-directed tension may occur. The other alternative is suggested by experiments of rock fracture under low and intermediate confining pressure, conditions satisfied in the shallow crust, in which dilatant cracks parallel to $\sigma_1$ may form. The first alternative requires the participation of lower crustal or upper mantle flow while the second alternative implies the transmission of collision-induced stress into the Strait. Although normal faulting could also occur in the outer-rise area due to the bending of the lithosphere (an implication of the thin-skinned hypothesis), we do not offer this particular interpretation because there is no evidence for the existence of active normal faults in the Strait that are parallel to the assumed plate boundary based on extensive petroleum company seismic profiles (e.g., Sun, 1985). Furthermore, the *T*-axis for the September 16, 1994 earthquake described earlier is perpendicular, not parallel, to the presumed subduction direction, inconsistent with the plate bending model.

It should be said that the proposed hypothesis



is still limited in scope. The lack of data below about 60 km prevents us including considerations regarding the processes in the upper mantle under the Taiwan orogen. For example, as a consequence of the formation of the root, rocks under a shallower thermal regime in the upper mantle must be pushed downward to greater depth (by 20–30 km), where the ambient temperatures are higher. Thus, we may expect it to form a positive density anomaly that could lead to 'delamination', a process that has been proposed in conjunction with orogeny (Bird, 1978; Molnar, 1988). Also, we did not deal with the potentially resolvable question of how the former subduction ceased and collision began. We can answer the question partly through a search for the remnant subduction zone either through seismicity or velocity anomalies. But until the seismic network is expanded to cover the Philippine Sea area east of Taiwan, a search is not possible. We shall expand the hypothesis in the future if warranted.

### 4.5. *Proposed falsification experiments of lithosphere collision models*

In the discussion above a number of implications are described and several of them can be subjected to tests. Such tests can be performed with existing data of which the PI's are not aware, or with experiments designed specifically to falsify various aspects of the hypothesis. In the following discussion we shall suggest an initial set of tests.

Although judging from the seismicity under the Coastal Range and through rheological considerations, the Philippine Sea plate near Taiwan appears to have been thickened, with the land-based seismic network, the locations of offshore earthquakes, their depths in particular, are not very well constrained. If the crust does not thicken at the margin of the Philippine Sea plate, then a major question arises: how is the shortening of the Philippine Sea achieved? The recently acquired data in this area (C.S. Liu, pers. commun., July 1996) will most probably provide a basis for testing. In any case, the intraplate deformation of the Philippine Sea plate near Taiwan is one of the major aspects of the collision tectonics.

One of the critical elements in the proposed model is the manner in which the Central Range was created. If the mid- to lower crust extrusion model is right, then the modern deformation of the Central Range as measured in leveling or vertical GPS surveys should indicate an overall more rapid uplift in the higher ranges. The long-term deformation should be recorded in the geologic structures in the Central Range as well. Thus detailed mapping of the Range will be highly desirable. To decipher the transition from the Western Foothills to the Central Range, from a rheologically sandwiched (brittle–ductile–brittle) region to a highly mobile region will be most interesting. Here, refraction and near-vertical incidence reflection studies will likely yield pertinent data to test whether there is a marked change in seismic velocities between the two units. By extruding the deeper rocks to shallower level the thermal regime will certainly have changed. The thermal gradient at shallow level must be drastically increased, but the thermal gradient in the mid-crust would have been decreased. In terms of thermal gradients near the surface, there are many hot springs in the Central Range (Chen, 1982), and the available heat flow measurements there do indicate higher values, but they are not corrected for topography. Heat flow measurements being difficult to make and interpret in areas of extreme relief, perhaps modern magnetotelluric measurements (Park et al., 1993) may be used to obtain electric conductivities, which can in turn be interpreted in terms of thermal structures.

One of the deductions of the hypothesis that is eminently falsifiable is the existence of the transition in southern Taiwan discussed above. Limited existing data do show that the anticlinal axis near Kaoshiung (Fig. 1) undergoes a turn (Sun, 1963) that is consistent with a left-lateral motion in the transition zone. Detailed work in this area is hampered by restricted access to some key outcrops, the lack of a good geologic map (the 1:50,000 map has not yet been completed) and much of the possible evidence is to be found under the Coastal Plain. Also, the seismicity there is less frequent than further north, and therefore will require more time before we can use seismicity and focal mechanisms to look at the nature of deformation there. Further accumulation of GPS data should also clarify the relative motions between the Hengchun Peninsula and the rest of the island. If the transition zone does not exist then the difference between what we think is the collision zone and the accretionary wedge does not exist, and a major part of the hypothesis has to be modified or abandoned.

Currently the tectonics of the Taiwan Strait and its relation to that in the Coastal Plain cannot yet be completely deciphered. We hypothesized that the flow in the crust or in the upper mantle are probably responsible for the generation of the N–S tensile stress that resulted in the graben formation. If so, there are probably certain flow patterns given the boundary conditions. To falsify the flow and the stress transmission model proposed, we can map the anisotropy in the area. Also, the distribution of active normal faults in the Strait and their orientations will enable us to decipher the relation between the Taiwan orogeny and the ongoing deformation in the Taiwan Strait. When data exchange across the Strait takes place, then such studies can be done.

## 5. Discussion and conclusion

In that Taiwan is a prime example of active arc–continent collision and that both an established knowledge base and extensive research infrastructure exist locally, further detailed studies can provide a sound basis for testing hypotheses on orogeny. Although this orogen is relatively compact, it is not simple, and extensive analyses of recently acquired data will evidently be the immediate step needed to advance further in our understanding. Attempts to apply the Popperian concepts of scientific investigation in the study of tectonics of Taiwan can help us focus our attention on key aspects of the tectonic problem.

As far as the Taiwan orogeny is concerned, we are faced with an unprecedented opportunity in understanding the dynamics of the Taiwan orogen. Of the many proposed experiments, the reflection profiling across the Central Range will probably be the most useful in obtaining a high-resolution image of the key components of the core of the mountain. Although the vertical boundary will not be clearly imaged, the boundary between the Central Range and the Foothills could be well delineated. The infrastructures exist in Taiwan to conduct such profiling. A long-term (on the order of a year) ocean-bottom seismometer (OBS) deployment in the offshore area of eastern Taiwan to record both local seismicity and teleseisms can provide data to study more clearly the intraplate tectonics of the collisional margin of the Philippine Sea plate. OBS deployment can also address the question, 'where did the subducted slab go?', using teleseismic tomography to search for a high-velocity zone in the mantle. Data on thermal structures are also very critical. Although magnetotelluric studies can provide some constraints, a few direct heat flow measurements will eventually be necessary.

More thorough testing will enable us to establish a better conceptual model. With such a model appropriate numerical simulations can then be formulated and conducted, thus allowing us to quantify estimates of the rate of uplift, the strain rate in different areas, etc. Inconsistencies with such modeling will indicate either the weakness of the model or the inadequacy of data, thus pointing out the need of further data taking. Such iteration should place the study of orogeny on a firm basis.

## Acknowledgements

This research came into focus when the senior author was on sabbatical leave from SUNY Binghamton in 1993 at the Institute of Earth Sciences (IES), Academia Sinica, in Taipei, Taiwan. A series of seminars on the tectonics of Taiwan co-convened with Dr. Y.H. Yeh was particularly stimulating. Discussions with Prof. Y.L. Yung of California Institute of Technology on science in general were useful in directing the senior author's queries. The senior author wishes to acknowledge the importance of the threatened system of sabbatical leaves. NSF grants EAR-8916159 to the senior author initiated this phase of the Taiwan research and INT-9513945 enabled him to complete it. Dr. Ray Russo's review of the manuscript greatly improved it.

## References


Barr, T.D. and Dahlen, F.A., 1989. Brittle frictional mountain building, II. Thermal structure and heat budget. J. Geophys. Res., 94: 3923–3947.

Benioff, H., 1955. Seismic evidence for crustal structure and tectonic activity. Geol. Soc. Am. Spec. Pap., 62: 61–95.

Biq, C., 1981. Collision, Taiwan-style. Mem. Geol. Soc. China, 4: 91–102.

Bird, P., 1978. Initiation of intracontinental subduction in the Himalaya. J. Geophys. Res., 83: 4975–4987.

Burchfiel, B.C. and Royden, L.H., 1985. North–south extension within the convergent Himalayan region. Geology, 13: 679–682.

Burchfiel, B.C., Chen, Z., Hodges, K.V., Liu, Y., Royden, L.H., Deng, C. and Xu, J., 1992. The south Tibetan detachment system, Himalayan orogen: extension contemporaneous with and parallel to shortening in a collisional mountain belt. Geol. Soc. Am. Spec. Pap., 269, 41 pp.

Byerlee, J.D., 1978. Friction of rocks. Pure Appl. Geophys., 116: 615–626.

Cardwell, R.K., Isacks, B.L. and Karig, D.E., 1980. The spatial distribution of earthquakes, focal mechanism solutions, and subducted lithosphere in the Philippine and northeastern Indonesian islands. In: D.E. Hayes (Editor), The Tectonic and Geologic Evolution of Southeast Asian Seas and Islands. Am. Geophys. Union, Geophys. Monogr., 23: 1–35.

Chai, B.H.T., 1972. Structure and tectonic evolution of Taiwan. Am. J. Sci., 272: 389–422.

Chang, M., 1992. Integrated geological and geophysical interpretation of Penghu sedimentary basin. Pet. Geol. Taiwan, 27:237–250.

Chen, C.H., 1982. Analysis of topographic effects on ascending thermal water in the Central Range of Taiwan. Proc. Natl. Sci. Council, 6:241–249.

Crespi, J., Chan, Y.-C. and Swaim, M. S., 1996. Synorogenic extension and exhumation of the Taiwan hinterland. Geology, 24: 247–250.

Dahlen, F. A. and Barr, T. D., 1989. Brittle frictional mountain building, 1. Deformation and mechanical energy budget. J. Geophys. Res., 94: 3906–3922.

Davis, D., Suppe, J. and Dahlen, F.A., 1983. Mechanics of fold-and-thrust belts and accretionary wedges. J. Geophys. Res., 88: 10,087–10,101.

England, P. and Molnar, P., 1993. Cause and effect among thrust and normal faulting, anatectic melting and exhumation in the Himalaya. In: P.J. Treloar and M.P. Searle (Editors), Himalayan Tectonics. Geol. Soc. London Publ., 74: 401–411.

Gong, S.Y., Lee, T.Y., Wu, J.C., Wang, S.W. and Yang, K.M., 1995. Possible links between Pliocene–Pleistocene reef development and thrust migration in the southwestern Taiwan. In: H.H. Tsien (Editor), International Conference and 3rd Sino–French Symposium on Active Collision in Taiwan, Program and Extended Abstracts. Geol. Soc. China Publ., pp. 113–119.

Grow, J.A. and Bowin, C.O., 1979. Multichannel seismic depth sections and interval velocities over outer continental shelf and upper continental slope between Cape Hatteras and Cape Cod. In: J.S. Watkins, L. Montadert and P.W. Dickerson (Editors), Geological and Geophysical Investigations of Continental Margins. Am. Assoc. Pet. Geol., Mem., 29: 65–83.

Hatcher, R.D. and Hooper, R.J., 1992. Evolution of crystalline thrust sheets in the internal parts of mountain chains, In: K.R. McClay (Editor), Thrust Tectonics. Chapman and Hall, London, pp. 217–233.

Ho, C.S., 1988. An Introduction to the Geology of Taiwan: Explanatory Text of the Geologic Map of Taiwan. Ministry of Economic Affairs, Taipei, 192 pp.

Hu, H.N. and Tsan, S.F., 1984. Structural study of the slate formation along the south link railroad, Taiwan. Spec. Publ. Central Geol. Surv., 3: 25–43.

Iwasaki, T., Hirata, N., Kanazawa, T., Melles, J., Suyehiro, K., Urabe, T., Moller, L., Makris, J. and Shimamura, H., 1990. Crustal and upper mantle structure in the Ryukyu island arc deduced from deep seismic sounding. Geophys. J. Int., 102: 631–651.

Kao, H. and Wu, F.T., 1996. The 16 September earthquake ($m_b = 6.5$) in the Taiwan Strait and its tectonic implications. Terr. Atmos. Ocean Sci., 7: 13–29.

Kohlstedt, D.L., Evans, B. and Mackwell, S.J., 1995. Strength of the lithosphere: constraints imposed by laboratory experiments. J. Geophys. Res., 100: 17585–17602.

Lallemand, S.E., Liu, C.S. and Lin, S.J., 1995. Behavior of the Ryukyu sliver in the wave of the indenting northern Luzon arc (east of Taiwan). In: H.H. Tsien (Editor), International Conference and 3rd Sino–French Symposium on Active Collision in Taiwan, Program and Extended Abstracts. Geol. Soc. China Publ., pp. 167–175.

Lee, C.R. and Chang, W.T., 1986. Preliminary heat flow measurements in Taiwan. In: Circum-Pacific Energy and Mineral Resources Conference, 4th, Singapore, Proceedings.

Lee, T.Q., Kissel, C., Barrier, E., Laj, C. and Chi, W.R., 1991. Paleomagnetic evidence for a diachronous clockwise rotation of the Coastal Range, Eastern Taiwan. Earth Planet. Sci. Lett., 104: 245–257.

Lee, T.-Y., Tang, C.-H., Ting, J.-S. and Hsu, Y.-Y., 1993. Sequence stratigraphy of the Tainan basin, offshore southwestern Taiwan. Pet. Geol. Taiwan, 28: 119–158.

Lee, T.Y., Hsu, Y.Y. and Tang, C.H., 1995. Structural geometry of the deformation front between 22°N and 23°N and migration of the Penghu Canyon, offshore of southwestern Taiwan arc–continent collision zone. In: H.H. Tsien (Editor), International Conference and 3rd Sino–French Symposium on Active Collision in Taiwan, Program and Extended Abstracts. Geol. Soc. China Publ., pp. 219–227.

Lee, W.H.K., Wu, F.T. and Jacobson, C., 1976. A catalog of historical earthquakes in China compiles from recent Chinese publications. Bull. Seismol. Soc. Am., 66: 2003–2016.

Lin, C.H. and Roecker, S.W., 1993. Deep earthquakes beneath central Taiwan: mantle shearing in an arc–continent collision. Tectonics, 12: 745–755.

Lin, S.C., 1994. Bathymetry and seismic Characteristics Offshore Eastern Taiwan, and its Tectonic Implication. M.S. Thesis, Institute of Oceanography, National Taiwan University, 77 pp.

Lyon-Caen, H. and Molnar, P., 1983. Constraints on the structure of the Himalaya from an analysis of gravity anomalies and a flexural model of the lithosphere. J. Geophys. Res., 88: 8171–8183.

Molnar, P., 1988. A review of geophysical constraints on the deep structure of the Tibetan Plateau, the Himalaya and the Karakoram, and their tectonic implications. Trans. R. Soc. London, A, 327: 33–88.

Nafe, J.E. and Drake, C.L., 1965. Density vs velocity curve. In: F.S. Grant and G.F. West (Editors), Interpretation Theory

in Applied Geophysics. McGraw-Hill Book Company, New York, pp. 199–200.
Park, S.K., Johnston, M.J.S., Madden, T.R., Morgan, F.D. and Morrison, H.F., 1993. Electromagnetic precursors to earthquakes in the ULF band: a review of observations and mechanisms. Rev. Geophys., 31: 117–132.
Popper, K.R., 1968. The Logic of Scientific Discovery. Harper Torchbooks, Harper and Row, New York.
Rau, R.J., 1992. Flexure Modeling and Taiwan Tectonics. Master thesis, State University of New York at Binghamton, 131 pp.
Rau, R.J. and Wu, F.T., 1995. Tomographic imaging of lithospheric structures under Taiwan. Earth Planet. Sci. Lett., 133: 517–532.
Rau, R.J., Wu, F.T. and Shin, T.C., 1996. Regional network focal mechanism determination using 3-D velocity model and SH/P amplitude ratio. Bull. Seismol. Soc. Am., in press.
Reed, D., Lundberg, N., Liu, C.S. and Kuo, B.Y., 1992. Structural relations along the margins of the offshore Taiwan accretionary wedge: implications for accretion and crustal kinematics, Acta Geol. Taiwan., 30: 105–122.
Rich, J.L., 1934. Mechanics of low-angle overthrust faulting as illustrated by Cumberland thrust block, Virginia, Kentucky and Tennessee. Amer. Assoc. Pet. Geol. Bull., 18: 1584–1594.
Salzberg, D.H., 1996. Simultaneous Inversion of Moderate Earthquakes Using Body and Surface Waves: Methodology and Applications to the Study of the Tectonic of Taiwan. Ph.D. Thesis, State University of New York, Binghamton, NY.
Seno, T., Stein, S. and Gripp, A.E., 1993. A model for the motion of the Philippine Sea plate consistent with NUVEL-1 and geological data. J. Geophys. Res., 98: 17941–17948.
Slemmons, D.B. and Depolo, C.M., 1986. Evaluation of active faulting and associated hazards. In: R.E. Wallace (Editor), Active Tectonics. U.S. Geol. Surv., Menlo Park, Calif., pp. 45–62.
Sun, S.C., 1963. The reef limestones and the geologic structures in the vicinity of Kaohsiung city, Taiwan. Pet. Geol. Taiwan, 2: 47–64.
Sun, S.C., 1985. The Cenozoic tectonic evolution of offshore Taiwan. Energy, 10: 421–432.
Suppe, J., 1976. Decollement folding in western Taiwan. Pet. Geol. Taiwan, 13: 25–35.
Suppe, J., 1980. Imbricate structure of western Foothills belt, south-central Taiwan. Pet. Geol. Taiwan, 17: 1–16.
Suppe, J., 1981. Mechanics of mountain building and metamorphism in Taiwan. Mem. Geol. Soc. China, 4: 67–89.
Suppe, J., 1984. Kinematics of arc-continent collision, flipping of subduction, and back-arc spreading near Taiwan. Mem. Geol. Soc. China, 6: 21–33.
Suppe, J., 1987. The active Taiwan mountain belt. In: J.P. Schaer and J. Rodgers (Editors), The Anatomy of Mountain Ranges. Princeton Univ. Press, Princeton, N.J., pp. 277–293.
Teng, L.S., 1990. Geotectonic evolution of late Cenozoic arc–continent collision in Taiwan. Tectonophysics, 183: 57–76.
Tsai, Y.B., 1986. Seismotectonics of Taiwan. Tectonophysics, 125: 17–37.
Tsao, S., Li, T.C., Tien, J.L., Chen, C.H., Liu, T.K. and Chen, C.H., 1992. Illite crystallinity and fission-track ages along the east central cross-island highway of Taiwan. Acta Geol. Taiwan., 30: 45–64.
Wu, F.T., 1970. Focal mechanisms and tectonics in the vicinity of Taiwan. Bull. Seismol. Soc. Am., 60: 2045–2056.
Wu, F.T., 1978. Recent tectonics of Taiwan. J. Phys. Earth, 26: S265–299.
Wu, F.T., 1996. A proposed transition between the collisional orogen and the accretionary wedge in southern Taiwan. Manuscript to be submitted.
Wu, F.T., Chen, K.C., Wang, J.H., McCaffrey, R. and Salzberg, D., 1989. Focal mechanisms of recent large earthquakes and the nature of faulting in the Longitudinal Valley of eastern Taiwan. Proc. Geol. Soc. China, 32: 157–177.
Yeh, Y.H. and Yen, H.Y., 1992. Bouguer anomaly map of Taiwan. Inst. Earth Sci., Acad. Sin., Taipei.
Yeh, Y.H., Lin, C.H., Liu, C.C., Yeh, H.Y., Huang, B.S., Liu, C.S., Wu, F.T. and Shi, R.C., 1995. Wide-angle deep seismic profiling in Taiwan. EOS, Trans. Am. Geophys. Union, F635.
Yen, H.-Y., Liang, W.-T., Kuo, B.-Y., Yeh, Y.-H., Liu, C.-S., Reed, D., Lundberg, N., Su, F.-C. and Chung, H.-S., 1995. A regional gravity map for the subduction–collision zone near Taiwan. Terr. Atmos. Ocean Sci., 6: 233–250.
Yu, S.B. and Chen, H.Y., 1994. Global positioning system measurements of crustal deformation in the Taiwan arc–continent collision zone. Terr. Atmos. Ocean Sci., 5: 477–498.
Zhao, W.L. and Morgan, W.J.P., 1987. Injection of Indian crust into Tibetan lower crust, a two-dimensional finite element model study. Tectonics, 6: 489–504.
Zwick, P., McCaffrey, R. and Abers, G., 1995. Earthquake moment tensor analysis from inversion of teleseismic body waves. Manuscript, RPI, Troy, New York, 118 pp.

**Publication Information**
*Tectonophysics* (ISSN 0040-1951). For 1997 volumes 265–278 are scheduled for publication. Subscription prices are available upon request from the publisher. Subscriptions are accepted on a prepaid basis only and are entered on a calendar year basis. Issues are sent by surface mail except to the following countries where air delivery via SAL is ensured: Argentina, Australia, Brazil, Canada, Hong Kong, India, Israel, Japan, Malaysia, Mexico, New Zealand, Pakistan, PR China, Singapore, South Africa, South Korea, Taiwan, Thailand, USA. For all other countries airmail rates are available upon request. Claims for missing issues must be made within six months of our publication (mailing) date. For orders, claims, product enquiries (no manuscript enquiries) please contact the Customer Support Department at the Regional Sales Office nearest to you:
**New York**, Elsevier Science, P.O. Box 945, New York, NY 10159-0945, USA. Tel: (+1) 212-633-3730, [Toll Free number for North American customers: 1-888-4ES-INFO (437-4636)], Fax: (+1) 212-633-3680, E-mail: usinfo-f@elsevier.com
**Amsterdam**, Elsevier Science, P.O. Box 211, 1000 AE Amsterdam, The Netherlands. Tel: (+31) 20-485-3757, Fax: (+31) 20-485-3432, E-mail: nlinfo-f@elsevier.nl
**Tokyo**, Elsevier Science, 9-15, Higashi-Azabu 1-chome, Minato-ku, Tokyo 106, Japan. Tel: (+81) 3-5561-5033, Fax: (+81) 3-5561-5047, E-mail: kyf04035@niftyserve.or.jp
**Singapore**, Elsevier Science, No. 1 Temasek Avenue, #17-01 Millenia Tower, Singapore 039192. Tel: (+65) 434-3727, Fax: (+65) 337-2230, E-mail: asiainfo@elsevier.com.sg

US mailing notice – *Tectonophysics* (ISSN 0040-1951) is published bi-weekly by Elsevier Science B.V. (Molenwerf 1, Postbus 211, 1000 AE Amsterdam). Annual subscription price in the USA US$ 2505 (US$ price valid in North, Central and South America only), including air speed delivery. Periodicals postage paid at Jamaica, NY 11431.
USA POSTMASTERS: Send address changes to *Tectonophysics*, Publications Expediting, Inc., 200 Meacham Avenue, Elmont, NY 11003.
Airfreight and mailing in the USA by Publications Expediting.



## NOTE TO CONTRIBUTORS

A detailed Guide for Authors is available on request. Please pay attention to the following notes:

*Language*
The official language of the journal is English.

*Preparation of the text*
(a) The manuscript should preferably be prepared on a word processor and printed with double spacing and wide margins and include an abstract of not more than 500 words.
(b) Authors should use IUGS terminology. The use of S.I. units is also recommended.
(c) The title page should include the name(s) of the author(s), their affiliations, fax and e-mail numbers. In case of more than one author, please indicate to whom the correspondence should be addressed.

*References*
(a) References in the text consist of the surname of the author(s), followed by the year of publication in parentheses. All references cited in the text should be given in the reference list and vice versa.
(b) The reference list should be in alphabetical order.

*Tables*
Tables should be compiled on separate sheets and should be numbered according to their sequence in the text. Tables can also be sent as glossy prints to avoid errors in typesetting.

*Illustrations*
(a) Illustrations should be submitted in triplicate. Please note that upon submission of a manuscript *three sets* of all photographic material printed *sharply* on *glossy paper* or as *high-definition laser prints* must be provided to enable meaningful review. Photocopies and other low-quality prints will not be accepted for review.
(b) Colour figures can be accepted providing the reproduction costs are met by the author. Please consult the publisher for further information.

*Page proofs*
One set of page proofs will be sent to the corresponding author, to be checked for typesetting/editing. The author is not expected to make changes or corrections that constitute departures from the article in its accepted form. To avoid postal delay, authors are requested to return corrections to the desk-editor, Mr. Herman E. Engelen, by FAX (+31.20.4852459\) or e-mail (h.engelen@elsevier.nl), preferably within 3 days.

*Reprints*
Fifty reprints of each article published are supplied free of charge. Additional reprints can be ordered on a reprint order form, which will be sent to the corresponding author upon acceptance of the article.

*Submission of manuscripts*
Three copies should be submitted to: Editorial Office *Tectonophysics*, P.O. Box 1930, 1000 BX Amsterdam, The Netherlands.
Submission of an article is understood to imply that the article is original and unpublished and is not being considered for publication elsewhere.
Upon acceptance of an article by the journal, the author(s) will be asked to transfer the copyright of the article to the publisher. This transfer will ensure the widest possible dissemination of information under the U.S. Copyright Law.
The indication of a fax and e-mail number on submission of the manuscript could assist in speeding communications. The fax number for the Amsterdam office is +31-20-4852696.
*Authors in Japan, please note*: Upon request, Elsevier Science Japan will provide authors with a list of people who can check and improve the English of their paper (before submission). Please contact our Tokyo office: Elsevier Science Japan, 1-9-15 Higashi-Azabu, Minato-ku, Tokyo 106; Tel. (+81) 3 5561 5032; Fax (+81) 3 5561 5045.
**THERE ARE NO PAGE CHARGES**

*Submission of electronic text*
In order to publish the paper as quickly as possible after acceptance authors are encouraged to submit the final text also on a 3.5″ or 5.25″ diskette. Essential is that the name and version of the wordprocessing program, type of computer on which the text was prepared, and format of the text files are clearly indicated. Authors are requested to ensure that apart from any such small last-minute corrections, the disk version corresponds exactly to the hardcopy.
If available, electronic files of the figures should also be included on a separate floppy disk.

Reprinted from

EARTH AND PLANETARY SCIENCE LETTERS

Earth and Planetary Science Letters 133 (1995) 517–532

# Tomographic imaging of lithospheric structures under Taiwan

Ruey-Juin Rau, Francis T. Wu

*Department of Geological Sciences State University of New York at Binghamton, Binghamton, NY 13902, USA*

Received 15 September 1994; accepted 23 March 1995

ELSEVIER

PUBLICATION INFORMATION

*Earth and Planetary Science Letters* (ISSN 0012-821X). For 1995 volumes 127–135 are scheduled for publication. Subscription prices are available upon request from the publisher. Subscriptions are accepted on a prepaid basis only and are entered on a calendar year basis. Issues are sent by surface mail except to the following countries where air delivery via SAL is ensured: Argentina, Australia, Brazil, Canada, Hong Kong, India, Israel, Japan, Malaysia, Mexico, New Zealand, Pakistan, PR China, Singapore, South Africa, South Korea, Taiwan, Thailand, USA. For all other countries airmail rates are available upon request. Claims for missing issues must be made within six months of our publication (mailing) date. Please address all your requests regarding orders and subscription queries to: Elsevier Science B.V., Journal Department, P.O. Box 211, 1000 AE Amsterdam, The Netherlands. Tel.: 31-20-4853642, fax: 31-20-4853598. *U.S. mailing notice: Earth and Planetary Science Letters* (ISSN 0012-821X) is published monthly by Elsevier Science B.V., Molenwerf 1, P.O. Box 211, 1000 AE, Amsterdam, The Netherlands. The annual subscription price in the U.S.A. is ca. U.S. $1788 (US$ price valid in North, Central and South America only) including air-speed delivery. Second class postage paid at Jamaica, NY 11431, U.S.A. *U.S.A. postmasters:* Send address changes to *Earth and Planetary Science Letters,* Publications Expediting, Inc., 200 Meacham Avenue, Elmont, NY 11003, U.S.A.
*Advertising information* Advertising orders and enquiries may be sent to: Elsevier Science B.V., Advertising Department, P.O. Box 211, 1000 AE Amsterdam, The Netherlands, tel.: +31-20-4853796, fax: +31-20-4853810. Courier shipments to: Molenwerf 1, 1014 AG Amsterdam, The Netherlands. *In the UK:* T.G. Scott & Son Ltd., attn. Vanessa Bird, Portland House, 21 Narborough Road, Cosby, Leicestershire, LE9 5TA, UK, tel.: +44-0116-2750521/2753333, fax: +44-0116-2750522. *In the USA and Canada:* Weston Media Associates, attn. Daniel Lipner, P.O. Box 1110, Greens Farms, CT 06436-1110, USA, tel.: +1-203-2612500, fax: +1-203-2610101.





ELSEVIER

Earth and Planetary Science Letters 133 (1995) 517–532

EPSL


# Tomographic imaging of lithospheric structures under Taiwan


Ruey-Juin Rau, Francis T. Wu

*Department of Geological Sciences State University of New York at Binghamton, Binghamton, NY 13902, USA*



Received 15 September 1994; accepted 23 March 1995



**Abstract**

Tomographic images of the crustal and mantle velocity structures under Taiwan are obtained by simultaneous inversion of local earthquake P-wave arrival times for hypocenters and P-wave velocity structures. In northern Taiwan, a high-velocity zone, coinciding with the Wadati-Benioff zone, can readily be identified as the subducted Philippine Sea plate. The imaged zone dips toward the north at an angle of 40° from a depth range of 20–55 to 100–130 km. An upper-mantle low-velocity wedge, ranging from 40 to 80 km in depth, exists above the subducted slab. Above this wedge is the Ilan Plain of northern Taiwan which lies at the west end of the Okinawa Trough, a well recognized back-arc basin; the crustal velocities under the Plain are also relatively low. The well-defined high-velocity zone and the low-velocity wedge provide some constraints on the thermal structures of the subduction system under northern Taiwan. In tomographic images across the central section of Taiwan, thickening of the crust and up-arching of the lower-crustal materials under the Central Range are commonly observed; the crust under the Western Foothills region is clearly thinner and the near-surface low-velocity layers are well developed. The structures under the Central Range show that although the Taiwan orogeny is quite young, a root, deeper in the north and shallowing to the south, has formed. The results of our tomography show that a significant portion of the lithosphere is involved in the Taiwan orogeny.


## 1. Introduction

The Taiwan mountain range was created by the collision between the Eurasian Plate and the Philippine Sea Plate (Fig. 1); the collision began at about 4 mybp [1]. The overall plate configuration in the vicinity of Taiwan, as defined by seismicity, is well understood [1,2]. The NW-dipping Ryukyu subduction zone becomes E–W-trending and N-dipping as it dives partially under northern Taiwan. The E-dipping North Luzon seismic zone extends northward to southern Taiwan. The central part of Taiwan, however, is underlain by only shallow seismicity (< 50 km) and a collision is taking place in this section. Near Taiwan, the relative plate motion between the Eurasian Plate and the Philippine Sea Plate is in the direction of N50°W and at an estimated rate of 7.1 cm/yr [3]. This motion is responsible for the collision tectonics of Taiwan.

The seismicity, the rate of uplift [4], and the geodetically measured deformation [5] all indicate that the ongoing tectonics in and around Taiwan is very active. Heretofore, relatively little was known about the crustal and upper-mantle structures, and, as a result, it is frequently assumed that the orogeny is a very superficial process, involving only the Cenozoic sediments in the upper part of the crust [6]. Previously, one-dimensional structures along several profiles were determined [2]; it was found that the crust under the eastern Coastal Range is relatively thin (20 km) and the velocities are close to those of a typical oceanic crust. In contrast, the crusts under the West-


0012-821X/95/$09.50 © 1995 Elsevier Science B.V. All rights reserved
*SSDI* 0012-821X(95)00076-3

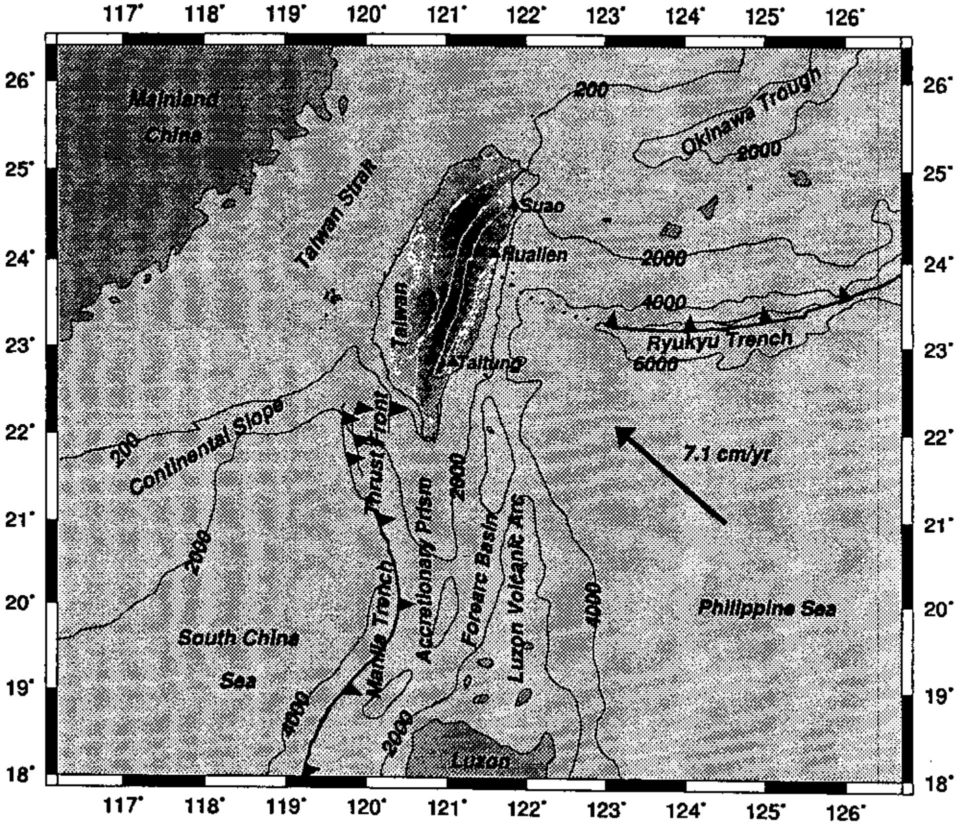


Fig. 1. Topography, bathymetry and tectonic setting of Taiwan and surrounding area (modified from [6]). The locations of the Ryukyu Trench to the east and the Manila Trench to the south are indicated. The vector of relative motion between the Philippine Sea plate and the Eurasian plate is shown by the arrow [3]. The dark area on the island is mountainous, with its highest peak at 3997 m. A small, triangular depression in northeastern Taiwan is the Ilan Plain. It lies at the west end of the Okinawa Trough. The Ryukyu Trench is assumed to continue westward along the dotted line [25]; in some previous work (e.g., [24]) the trench has been assumed to bend sharply northward near Taiwan and connect to Suao. The main geological divisions of Taiwan are demarcated by white lines. The isobaths (in m) outline the morphology of the Chinese continental shelf, slope and the other features.

Fig. 2. Map (top) and 3-D (bottom) views of three grid configurations used in our 3-D inversions. (a) EW–NS oriented grid system for the northern third of Taiwan. (b) Grid system with the horizontal orthogonal directions parallel (N20°E–S20°W) and perpendicular (S70°E–N70°W) to the strike of the island in the northern two-thirds of Taiwan. (c) EW–NS grid system for the whole island. ▲ = CWBSN and TTSN seismic stations; ○,● = original earthquake locations used in each system for map and 3-D views, respectively; ● = nodes (points where the lines cross) in the map view, at the intersections of the grid lines in the 3-D view. $A$–$A'$ through $F$–$F'$ indicate the positions of the tomographic profiles shown in Fig. 4. The selected sections are shaded vertically in the 3-D views. The geological provinces of Taiwan are: $I$ = Coastal Plain (CP); $II$ = Western Foothills (WF); $III$ = western Central Range (WCER); $IV$ = eastern Central Range (ECER); $V$ = Longitudinal Valley (LV); $VI$ = Coastal Range (COR).



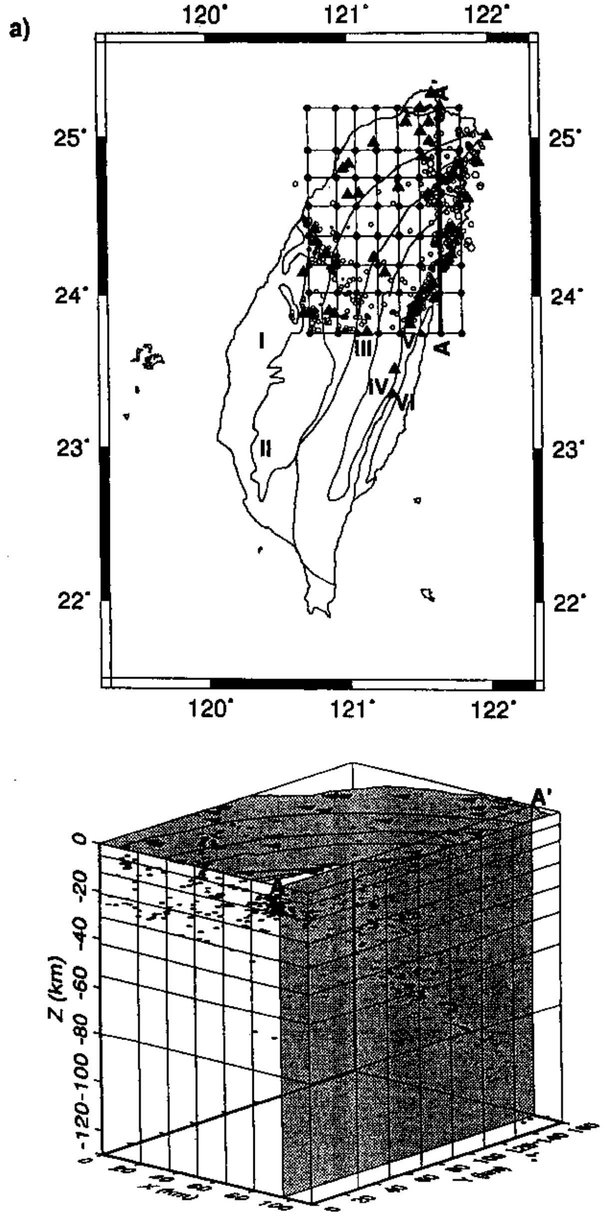

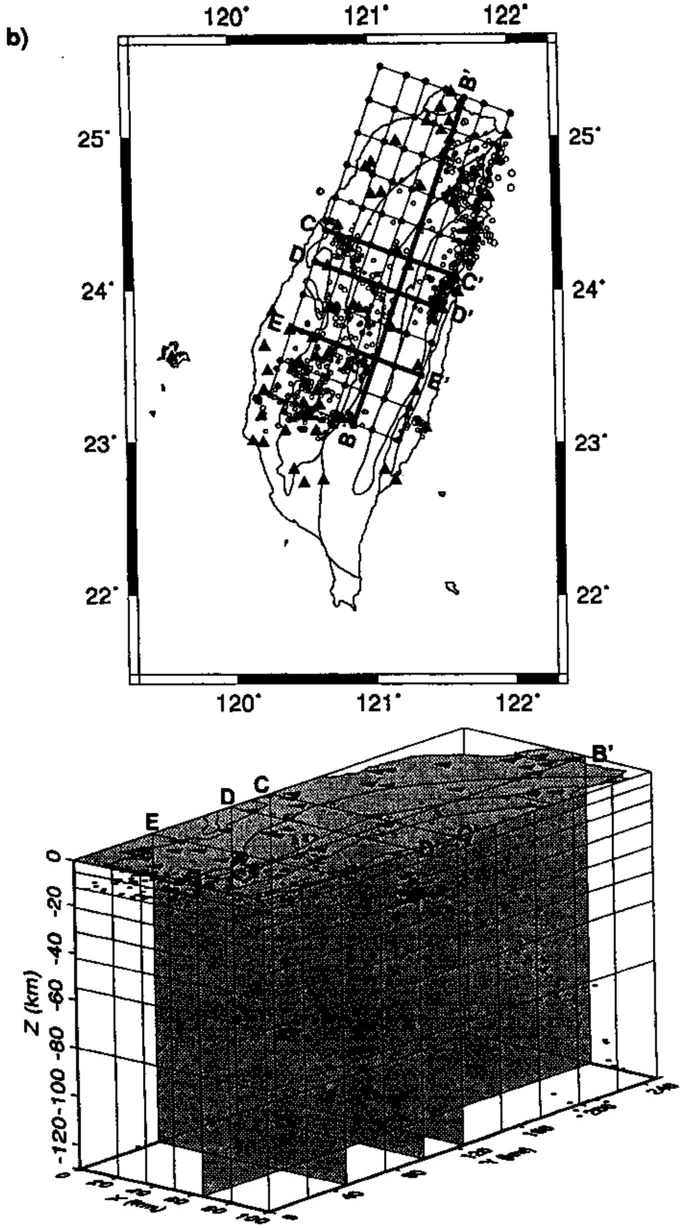


Fig. 2 (continued).



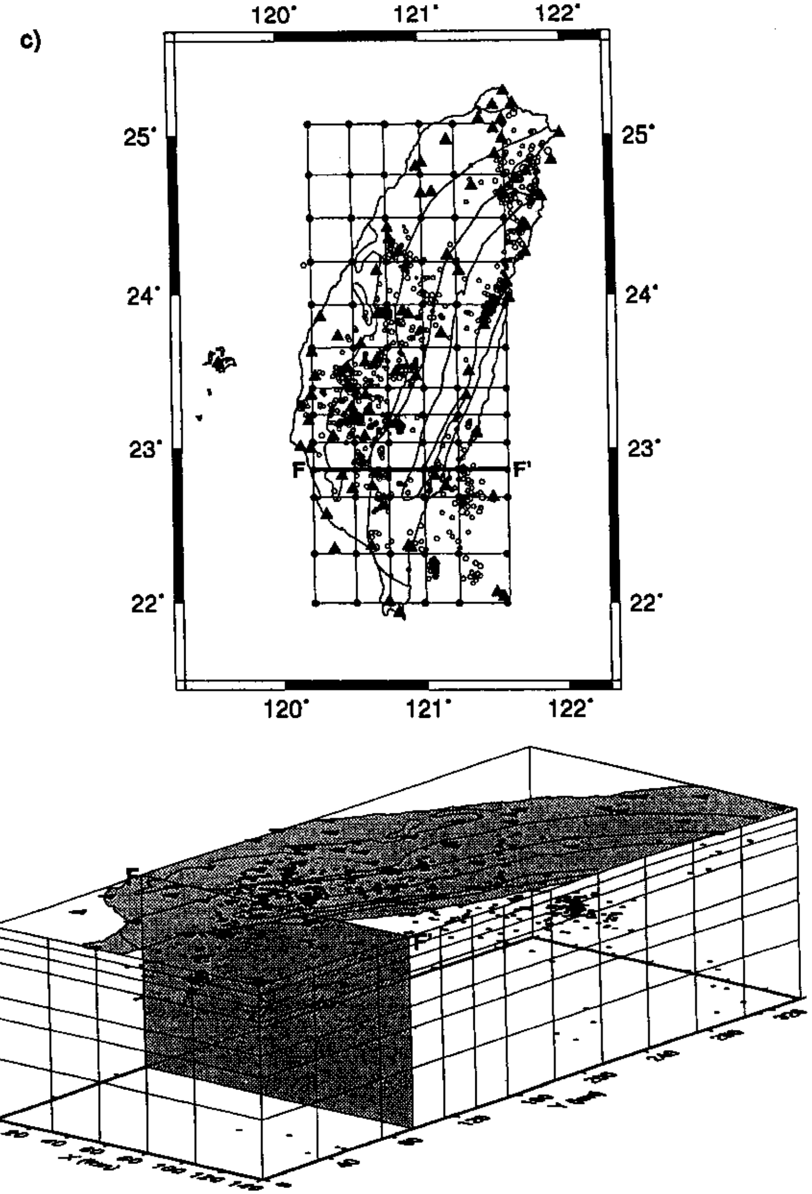


Fig. 2 (continued).

ern Foothills and the Central Range are both continental in nature, but the Moho under the Foothills is about 25 km and that under the Central Range is deepened to about 34 km. Three-dimensional velocity structures under Taiwan were determined by Roecker et al. [7] and Yeh et al. [8]. The resolution of these studies was limited by the sparse network and the precision of arrival time data. Nevertheless, Yeh et al. were able to define a shallow (< 6 km) low-velocity zone under the Ilan Plain area of northern Taiwan, and Roecker et al. mapped large-scale velocity anomalies under the whole island. But much of this relatively small and highly complex collision zone has not yet been mapped in any detail. We now attempt to study the subsurface structures under Taiwan in greater detail. Through this work, we wish to address the following two tectonics-related problems.

First, although the existence of the subduction system under northern Taiwan has been known for some time, some aspects of it remain unclear. For example, in the absence of detailed offshore multichannel seismic data, it is not yet possible to place the intersection of the "trench" with the island based on diffuse seismicity; this is necessary in order to know the precise geometry of the interacting plates near Taiwan. With tomography we can map the subsurface configuration of the subduction zone and extrapolate it for a short distance to the surface to find the "trench". Also, the Okinawa Trough, a back-arc basin, extends morphologically southwestward into northern Taiwan; the Trough narrows westward to form the triangular Ilan Plain, with its opening to the east. Judging from focal mechanisms (e.g., [1]), N–S extension is taking place under and offshore of the Plain. It appears that a back-arc basin is being formed in northern Taiwan. If so, tomographic images of northern Taiwan will allow us a rare opportunity to study the structures under a nascent back-arc basin in some detail.

The second problem is the search for deep structures under the Central Range associated with the collision tectonics. As the collision is younging toward the south [9], changes in subsurface structures from northern to southern Taiwan may show the manner in which the crust responds to tectonic deformation as a function of time. The crustal structures provide undoubtedly the best records of the large-scale strain sustained in the mountain building processes. In the thin-skinned tectonics modeling of the Taiwan orogeny [6], little thickening of the crust is expected, and the orogeny involves only Tertiary sediments from the Coastal Plain to the Central Range. But the existence of the sedimentary wedge extending across the Central Range has never been demonstrated and the passive role of the crust and upper mantle in the process is also assumed. Although we know from earlier work [2] the general changes in crustal structures across the island, details are lacking. Through tomography we wish to determine whether there is a deepening sedimentary wedge under the Central Range [6], and whether any significant structures exist in the crust and the upper mantle that might be related to the orogeny.

Detailed tomography is made possible by the recent expansion, in 1991, of the telemetered network on Taiwan and its neighboring islands (Fig. 2). Besides providing improved detection, the digitally recorded data also made phase identification and picking more efficient. A dataset, consisting of seismograms recorded for three and a half years, can now be used for tomographically imaging the deep structure under the Taiwan area. We found the body-wave tomographic imaging method as formulated by Thurber [10,11] to be quite suitable for this work.

Insofar as Taiwan has been considered a typical example of arc–continent collision orogen [12], a thorough understanding of the physical environment in which the orogenic processes are taking place is obviously important. A tomographic study of the lithospheric structures under Taiwan will provide us not only important constraints on the modeling of the Taiwan orogeny in particular, but will also lead us to a general understanding of the plate interactions and mountain building.

## 2. Data and method

The seismograms used in this study are recorded by the combined Central Weather Bureau Seismic Network (CWBSN) and the Taiwan Telemetered Seismographic Network (TTSN); it has a total of 75 stations (see Fig. 2). Prior to 1994, the TTSN had one component (vertical) stations; they have since been merged into the CWBSN and now are all



equipped with three-component short-period sensors. Out of the total 24,312 events located by the combined network between March 1991 and July 1994, 1197 events were chosen for this study. The event selection criteria were: (1) the earthquakes having arrivals recorded at more than 8 stations; and (2) the largest azimuthal gap being less than 180° between stations, except for the deep events in the subduction zone immediately northeast of the island. The P and S arrival times for the events chosen were checked and reread, especially for events in the subduction zone under northern Taiwan.

In our inversion, the P-wave velocities at grid points in a three-dimensional space are sought. Because of the specific station and event locations given, a particular choice of 3-D grids will cause some space between grids to be illuminated and others untouched. In order to examine different tectonic features in more detail, three different grid configurations (Fig. 2) were set up for the velocity parameterization in the three-dimensional velocity inversion. They are: (a) a EW–NS oriented grid system for the northern third of Taiwan; (b) a grid system with the horizontal orthogonal directions parallel (N20°E–S20°W) and perpendicular (S70°E–N70°W) to the strike of the island in the northern two-thirds of Taiwan; and (c) a EW–NS grid system for the whole island. We modeled only P waves in the present study. The number of the earthquakes and P-wave arrivals used in this study for three different areas are shown in Table 1.

Table 1
Key parameters and results relevant to the 3-D inversions

| Area | Number of Earthquakes | Number of P Arrivals | $V_p$ Damping | Initial Weighted RMS residual (seconds) | Final Weighted RMS residual (seconds) |
|---|---|---|---|---|---|
| Northern Taiwan | 510 | 8058 | 40 | 0.253 | 0.145 |
| North-Central Taiwan | 939 | 20,565 | 120 | 0.290 | 0.174 |
| Whole Taiwan | 1008 | 21,110 | 80 | 0.271 | 0.173 |

For each grid system, a one-dimensional velocity model is first obtained by a simultaneous inversion of both a layered velocity structure and the hypocentral locations [13], and it is used as the starting model for the tomographic inversion. In the simultaneous inversion [10,11,14], a damped, linear, least-squares inversion algorithm was used. Because the scale of computing involved is quite large, Pavlis and Booker's [15] method was used to decouple the hypocenter locations and the velocity structure determination in each step. Within each step we allow five iterations in the hypocenter location. The step is repeated until the result of the F-test shows that the change in variance is no longer significant; it usually takes six to seven steps. The velocity and its partial derivative at each discrete point in the 3-D model are calculated by linear interpolation from the surrounding eight grid points. The resulting velocity model is piecewise continuous and appropriate for modeling the complex tectonic environment in our study area. For the traveltime calculation, approximate ray-tracing algorithms were used to determine an initial minimum-time circular ray path connecting the source and receiver [10], and, through an iterative pseudo-bending approach [16], to adjust the ray path for a better approximation of the true path, which was in accord with the local velocity gradient.

To quantify the "goodness-of-fit" of the model parameters, the model standard error and spread function [17,18] are calculated. The model standard error is an estimate of how the data error is mapped

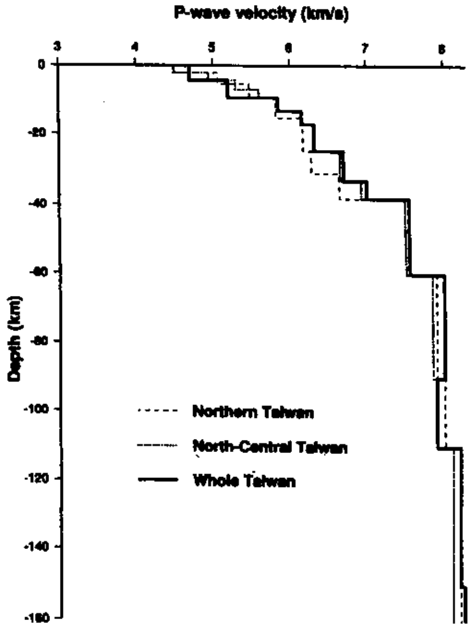


Fig. 3. One-dimensional P-wave velocity models for northern, north-central, and the whole of Taiwan obtained by simultaneous inversions for hypocenters and layer structures.

into the model error. A zero spread function implies a perfectly defined parameter, whereas large spread functions correspond to parameters having broad kernel shapes and small values of the resolving kernel.

To test the validity of our results, we ran inversions with a range of damping values. In the "spread-versus-the-standard-error" plot, the standard error initially decreases sharply when damping is increased, and then it decreases more slowly after the damping reaches a certain value. We define the optimum value for damping as a value in the vicinity of this transition. Thus, we seek compromise solutions that have a reasonable and standard error [17]. Solutions with damping values much lower than the adopted optimum value tend to be more oscillatory. For the inversions with the higher damping values, the velocity solution becomes highly smoothed.

## 3. Tomographic imaging results

The one-dimensional models obtained from 1-D inversions for the three selected grid configurations



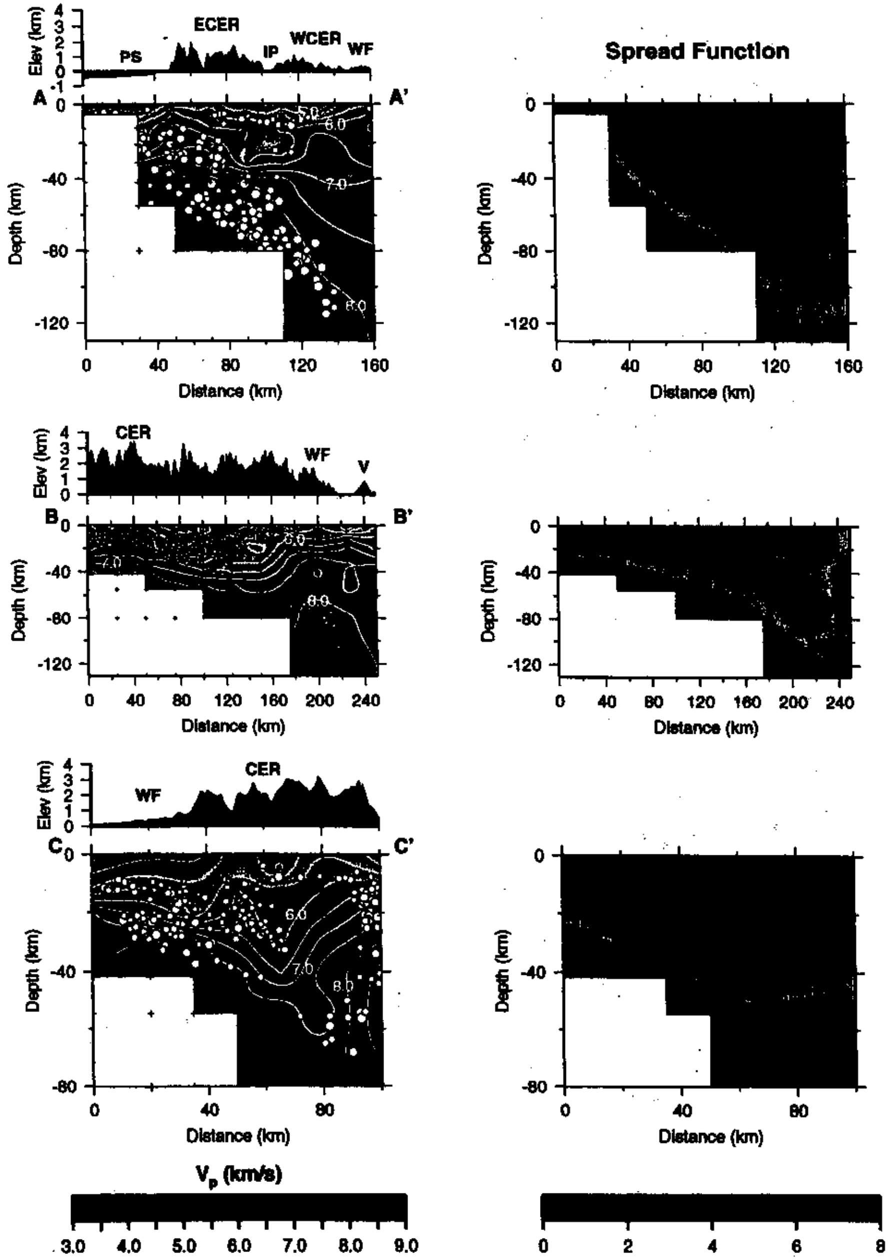


Fig. 4. Tomographic profiles and their corresponding spread functions; the locations of the profiles are shown in Fig. 2a–c. The P-wave velocity distributions are shown on the left and the spread functions are shown on the right. The velocity contour interval is 0.5 km/s. O = relocated hypocenters including events within ±1 grid space of the profile; + = locations of the nodes. White areas mark unsampled regions. The topography corresponding to each profile is shown on top of the velocity section. *PS* = Philippine Sea; *ECER* = eastern Central Range; *IP* = Ilan Plain; *WCER* = western Central Range; *WF* = Western Foothills; *V* = Tatun volcano group; *CP* = Coastal Plain; *COR* = Coastal Range. Note that profiles are not plotted on the same scale; in particular, *B–B'* is plotted at about 50% of the other profiles-the hypocenters shown in *B–B'* appear to be smaller in comparison with those shown in other profiles.

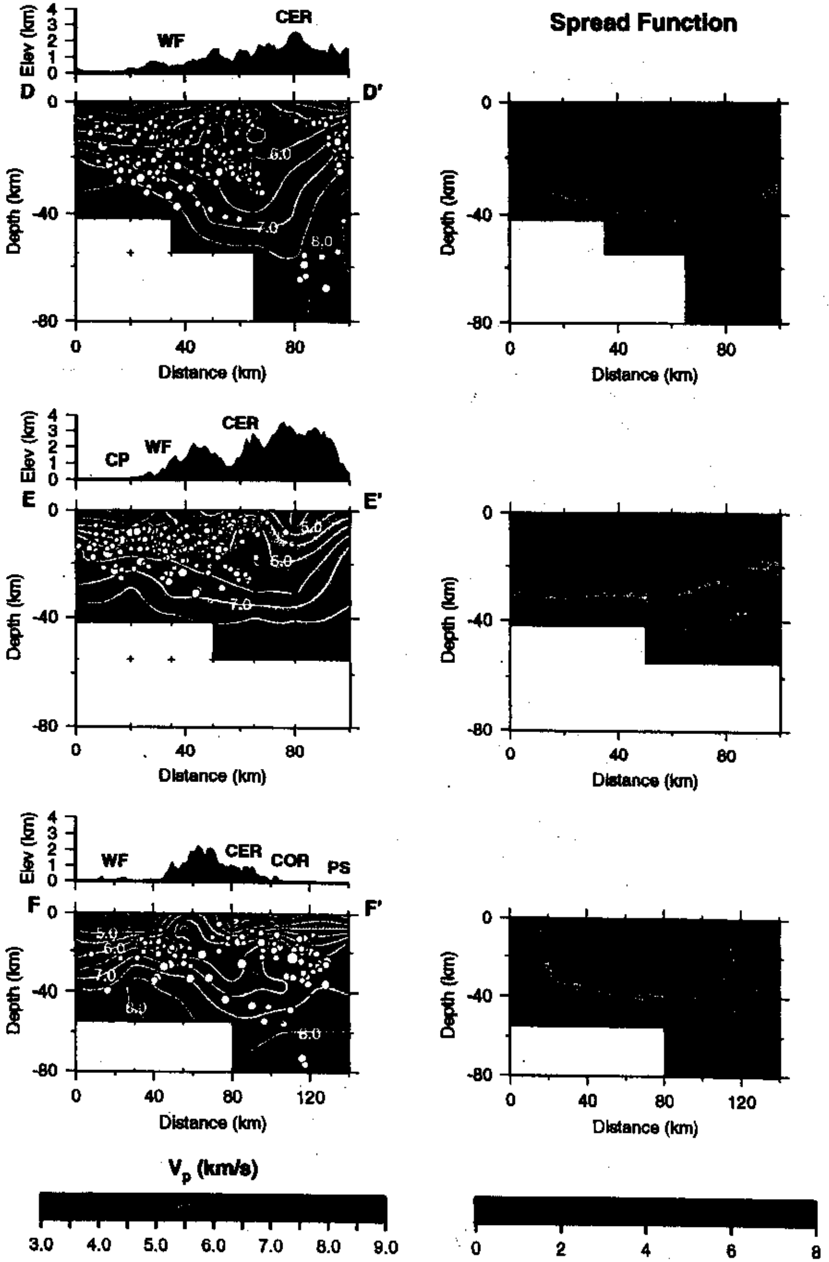


Fig. 4 (continued).



are shown in Fig. 3. The models for the northern two-thirds, and for the whole island are quite similar, as can be expected by the large overlap in their area coverage, although the events under the southern third of the island were not used in deriving the north-central Taiwan model. The northern Taiwan model is clearly different from the other two; 40 km can be taken as the Moho depth, where the $P_n$ velocity is about 7.6 km/s. The weighted root mean square (RMS) arrival time residuals obtained using these 1-D models are 0.253, 0.290 and 0.271 s for northern Taiwan, north-central Taiwan and the whole island, respectively.

The 1-D models are used as initial models for our 3-D inversions. At the end of six to seven iterations, the RMS residuals decreased from the values listed above to 0.145, 0.174 and 0.173 s, respectively. These are slightly higher than the overall estimated reading error of 0.07 s. The optimal P-wave velocity damping values chosen are listed in Table 1 for the three different areas. For the final results, the calculated average model standard errors are 0.04, 0.02 and 0.02 km/s for the areas of northern Taiwan, north-central Taiwan and the whole Taiwan, respectively. These errors may underestimate the actual error by 100%, as shown by Thurber [19], using synthetic tests. Thus, the average errors in absolute velocity of the final models of the current study may range up to 0.04–0.08 km/s. For most of the earthquakes, the resulting hypocenters in our 3-D inversions deviate from their initial locations by less than 2 km horizontally and 5 km vertically. For earthquakes below 80 km, or just outside the seismic network, the deviation may be as much as 10 km horizontally and 15 km vertically. In terms of absolute locations, the average errors of earthquake location are 3 km horizontally and 5 km vertically. For some deeper earthquakes, and earthquakes occurring just outside the network, the location errors range up to 10 km horizontally and 15 km vertically.

Our 3-D results are displayed in a series of profiles; their positions are marked in Fig. 2a–c. The profiles (Fig. 4) are chosen to show the major variation in velocity structures under Taiwan. The hypocenters shown in Fig. 4 have been relocated. The spread function for each profile is also presented to provide a basis for judging the spatial resolution of the cross-section [18]. In this study, we consider the acceptable spread function to be 5.0. In each of the profiles and the spread function plot the white areas mark the unsampled regions.

### 3.1. Northern Taiwan profile (A–A′)

The most prominent feature in the subsurface P-wave image of northern Taiwan is the inclined high-velocity zone (A–A′, Fig. 4). In section A–A′, this zone is mapped at a depth range of 20–55 km, starting at about 45 km on the distance axis (corresponding to 24°N, 121.6°E), and continuing northward with a shallow dip (< 20°) for 40 km, before it dives more steeply northward with a dip of 40° from a depth range of 40–80 to 100–130 km. The velocities in the subduction zone are 8.0–8.4 km/s, or about 3–8% higher than the 1-D average starting model in the depth range of 40–130 km. Also clear in this profile is the low-velocity wedge above the high-velocity zone, ranging from 40 to 80 km in depth. The velocities within the wedge are about 6.9–7.5 km/s, or 4–8% lower than the 1-D model. Above the wedge is a crustal (< 30 km) low-velocity zone (5.7 km/s or −4% on the average), under the Ilan Plain of northern Taiwan. In the upper 10 km, high P-wave velocities (5.0–6.2 km/s or 4–12% higher than that of the 1-D model) are found under the eastern Central Range, where high-grade metamorphic rocks crop out, and low P-wave velocities (4.0–5.5 km/s, or 4–12% higher) are found under the western Central Range. Note that the Wadati-Benioff zone, as defined by seismicity, coincides with the inclined high-velocity zone under northern Taiwan; this correlation renders the straightforward interpretation of the high-velocity zone as the subduction zone.

### 3.2. S20°W–N20°E profile (B–B′) (along the ridge of the Central Range)

The northern end of this profile coincides with that of profile A–A′; it diverges by 20°, clockwise, from A–A′. The point at which this profile crosses the low-velocity wedge it is 15 km west of the corresponding point on profile A–A′. This profile clearly images the structures under the ridge of the Central Range. In the north (to the right of the 170–190 km mark in B–B′), the westward extension of the N-dipping high-velocity zone and the low-velocity upper-mantle wedge observed in $A$–$A'$ can be discerned. While the velocities in the high-velocity zone in the two profiles are about the same, the velocities in the low-velocity wedge in profile $A$–$A'$ are noticeably lower than those in profile $B$–$B'$ ($-4$ to $-8\%$ vs. 0 to $-2\%$). The most striking features in $B$–$B'$ are the thickening of the lower-velocity upper structures (above a depth of 40 to 55 km) under the higher elevations to the left of the 170 km mark along the distance axis and the gradual thinning of this structure further south (to the left in $B$–$B'$, Fig. 4). The implication of this observation in terms of tectonics is quite interesting as will be discussed below. Earthquakes in this section occur diffusely in the upper 40 km and within the inclined high-velocity zone; the middle part of the Central Range and the low-velocity wedge, however, are nearly aseismic.

### 3.3. N70°W–S70°E profiles, C–C′, D–D′, E–E′ and F–F′ (perpendicular to the strike of the island)

The most prominent feature in these sections (profiles $C$–$C'$ through $F$–$F'$) is the thickening of the crust under the higher elevations of the Central Range, except in southern Taiwan (profile $F$–$F'$), where the deepest part is offset to the east. This thickening is much more pronounced in the north ($C$–$C'$ and $D$–$D'$) where low-velocity materials extend to a depth of about 75 km; this low-velocity feature was also observed to some extent by Roecker et al. [7], but due to the larger block size used in their work, the velocity contrasts are much attenuated. The high velocities below about 20 km in the eastern part of the $C$–$C'$ and $D$–$D'$ profiles are in sharp contrast to the low-velocity root in the west; the contact between them is quite steep. Toward the south, although the thickening is still substantial along profile $E$–$E'$, it is noticeably less, and the lateral extent of the low-velocity crustal root is seen to have decreased in profile $F$–$F'$, in comparison to the three profiles to the north. Also consistently seen in these profiles are the relatively high velocities in the top 15 km under the Central Range, relative to velocities under the Foothills and the Coastal Plain; the 5.5 km/s contours in all four profiles rise under some part of the Range, although not necessarily the highest part. The thickness of the low-velocity materials (< 5.0 km/s) under the Foothills and the Coastal Plain imaged in these sections remain nearly constant. The earthquakes shown in these sections occur mostly in the upper 40 km under the Western Foothills and in the top 40–70 km, being deeper toward the north, under the eastern Central Range. The middle part of the Central Range is nearly aseismic.

An additional feature in the eastern part of profile $F$–$F'$ (Fig. 4) is the high-velocity zone, at a depth range of 15–50 km, under the Coastal Range and the Philippine Sea, between the 100 and 140 km marks on the distance axis. Note that the seismicity within this high-velocity zone is quite high. This profile is located just at the point where the subduction zone in southern Taiwan becomes visible based on seismicity. Thus, the high velocity observed at a depth range of 55–80 km in the eastern part of this profile may be related to this subduction zone; in fact, the seismicity shown in $F$–$F'$ (Fig. 4) also suggests this relationship.

## 4. Discussions

The 3-D velocity structures under Taiwan obtained by tomographic inversion present details of the crust and upper mantle that are key to the understanding of Taiwan tectonics. Of the easily identified features, the inclined high-velocity zone under northern Taiwan (profiles $A$–$A'$ and $B$–$B'$, Fig. 4) evidently corresponds to the subduction zone mapped previously by seismicity alone. In these profiles, zones of high velocity and the seismicity superpose. The number of earthquakes in the western zone, however, is quite small, yet the increase in velocities in these two locations is roughly the same. In neither profile is the underside of the slabs well illuminated, because the first P arrivals travel through the high-velocity slab -this is a particular problem in using local earthquake data for tomography. In terms of studying the low-velocity wedge above the subduction zone, Taiwan provides an interesting locale. The back-arc basin is evidently alive, and probably very young, judging by the presence of $M > 6$ normal-faulting earthquakes in the southwestern terminus of the Okinawa Trough offshore of Ilan [1] and



the rapid subsidence of the Ilan Plain [20]. The area of low velocities in $A$–$A'$ is more extensive and the values are lower than those in profile $B$–$B'$, just 15 km to the west. Both profiles intersect areas with recent volcanism, but $B$–$B'$ is placed to the west of the tip of the triangular-shaped Ilan Plain, not yet reached by the westward propagating Okinawa Trough. The juxtaposition of the low-velocity mantle wedge and the high-velocity slab is quite similar to those in the northwest Pacific [21], Alaska [22] and Japan [23]. Due to a lack of stations offshore of northern Taiwan, the northward extension of the mantle wedge cannot be mapped adequately along $A$–$A'$, but in profile $B$–$B'$ the velocity seems to increase near the northern end, signifying the termination of the low-velocity wedge.

One of the important questions in studying the Taiwan collision is the location of the trench near Taiwan. Since the compression is at its maximum where the two colliding plates are fully engaged, and it diminishes as the Philippine Sea Plate begins its northward subduction, this location determines where mountain building is taking place. Because of the disappearance of the bathymetric low associated with the Ryukyu Trench 100 km east of Taiwan, little evidence is available heretofore concerning the westward continuation of the Trench; it has been placed as far north as Suao [24], but, generally, it is believed to be near Hualien (e.g., [25]) (Fig. 1). Although seismicity defines the general plate configuration quite well, it is too diffuse for defining where the plate starts to bend. Also, between the end of the Ryukyu Trench and Taiwan there had not been any normal faulting earthquakes, which are associated with plate-bending near the trench [1]. By extrapolating the upper limit of the high-velocity zone to the south ($A$–$A'$, Fig. 4), the intersection of the "trench" with the island is located by our tomographic results at approximately 23.8°N. The collision-induced orogeny should gradually diminish north of this point. It is gradual because the finite plate thickness ensures that the total disengagement of the subducting Philippine Sea plate from the Eurasian plate will take a finite distance to complete. With a plate thickness

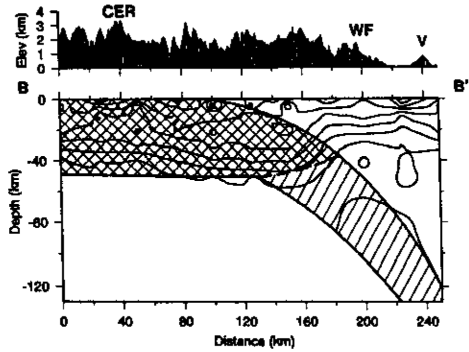


Fig. 5. Schematic diagram showing the position of the subducting Philippine Sea plate relative to the location of the mountains and its crustal root as indicated in profile $B$–$B'$ (Fig. 4). The subducting plate boundary is about 35 km east of the profile $B$–$B'$. The crosshatched area is the section in which the Eurasian and the Philippine Sea plates are fully engaged in collision. As the subducting plate dives further into the upper mantle, there is no longer any compression exerted on the Eurasian plate. Note that the average elevation on this profile remains nearly constant between 0 and 170 km on the distance axis. The elevation decreases gradually beyond 170 km.

of 50 km and an average dip of 30°, say, it will take 100 km. The situation is schematically illustrated in Fig. 5, in which an idealized subduction zone is superposed on the velocity contours in profile $B$–$B'$ (Fig. 4). The crosshatched area is the section in which the Eurasian and the Philippine Sea plates are fully engaged in collision, and to the north, where the subducting plate dives further into the upper mantle, no compression is exerted on the Eurasian plate.

Of great importance to the understanding of the Taiwan orogeny is the imaging of the relatively high-velocity region in the upper 10–15 km under the Central Range. In the "thin-skinned" modeling of Taiwan [6], the Central Range should be underlain by the deepest part of a tapered wedge consisting mainly of Tertiary sediments, and therefore should appear as a continuation of the upper-crustal low-velocity zone under the Western Foothills. In the images (Fig. 4) the upper-crustal high-velocity feature under the Central Range is seen to be continuous with the lower-crustal layer, which is generally thickened to form a "root" under the high elevations of the Central Range. Thus the formation of the

[1] Such an earthquake did take place on May 24, 1994, located at 24.04°N and 122.34°E (S. Sipkin, pers. commun., 1994).

Central Range appears to be resulting from up-arching of the pre-Tertiary basement and the lower-crustal materials, as well as the downwarping of the lower crust. In profile $C–C'$, high-velocity materials are seen to extend to the surface on the eastern end of the profile, where pre-Tertiary high-grade metamorphic rocks crop out. The high-velocity zones under the eastern Central Range imaged in profiles $C–C'$ and $D–D'$ are somewhat intriguing. The velocities in these zones are similar to those in the high-velocity zone under the Western Foothills and the Central Range, but the fact that they start as shallow as 20 km and are next to the Philippine Sea plate makes us suspect they are part of the oceanic lithosphere. The seismicity in this zone is also notably higher than in its neighboring area to the west. In profiles $C–C'$ and $D–D'$ the low-velocity root is seen to be quite deep, with the 7.5 km/s contour at around 55–65 km. How these deep roots form is a question worth exploring. Was it formed simply by crustal thickening or did the thickening lead to the breaking of the upper mantle lid and thus allowing the intrusion of the asthenosphere? With available data we cannot answer these questions with any certainty, but with an accumulation of teleseismic P-wave data, recorded by the network since late 1994, it can be studied in the future.

The variation of the extent of the root can also be seen from profile $B–B'$ (Fig. 4); using the 7.5 km/s contour as a marker, the root under the ridge of the Central Range is seen to decrease from a maximum of 55 km near the 160 km marker in $B–B'$ to about 40 km near the southern end of the profile. It is commonly agreed that because of the obliqueness of the collision that created Taiwan, the orogeny started in the north and propagated southward [6,9]. Lee et al. [9] placed the initial contact near the northern end of the Coastal Range, starting at about 4 my BP, and the collision is now proceeding further south from the southern end of the Coastal Range. If so, we should expect the mountains in the north to be more mature, with perhaps more of an extensive root, than in the south (near Taitung, see Fig. 1). The slow decrease southward of the root is most probably an expression of this process.

To further understand the imaged lateral variations of seismic velocity in the upper mantle we need to evaluate the velocity changes due to changes in composition and melt content of the mantle material or from changes in ambient pressure and temperature. In terms of composition change, changes in $V_p$ are related to the amount of basalt melt removal from the mantle. Studies [26,27] show that, with 10% basalt depletion, $V_p$ increases by $\sim 0.003$ km/s for upper mantle rocks; this is negligibly small. However, a 3–6% melt by volume may lead to a 5–10% decrease in $V_p$ [28], the aspect ratio of the cracks being the key factor determining the exact amount of variation. For the two ambient factors, temperature variations may cause a 0.04–0.06 km/s change in $V_p$ per 100°C, based on $\partial V_p/\partial T = -3.93 \times 10^{-4}$ km/s/°C [29] and $-6 \times 10^{-4}$ km/s/°C [30]. At confining pressures from 6 kbar ($\sim 18$ km) to 30 kbar ($\sim 90$ km), variations in pressure may cause up to 0.015 km/s change in $V_p$ per 1 kbar ($\sim 3$ km) [30,31]. The preceding values are for mantle rocks.

For the subduction system in northern Taiwan ($A–A'$, Fig. 4), the average absolute P-wave velocities are 8.2 km/s in the slab and 7.2 km/s in the mantle wedge (or $+6\%$ and $-6\%$ relative to the 1-D model) at depths of 50–100 km. The positive velocity anomaly can be explained readily by the subduction of cold lithosphere into the hot upper mantle. Given the Eurasian Plate–Philippine Sea Plate plate motion of 7.1 cm/yr in the direction of N50°W [3], the Philippine Sea Plate slab velocity is 3 cm/yr in the N20°E direction. Taking 40° as the dip and 60 km as the thickness of the slab, with values for other parameters and heat energy sources adapted from Creager and Jordan [32], the calculated average temperature contrast between the slab and the ''normal'' mantle is about 600°C at depths between 50 and 100 km, corresponding to a 0.24–0.36 km/s (3–5%) change in $V_p$. Intraplate deformation or escape of the Philippine Sea Plate [1] may speed up the subduction, but, even by increasing the slab velocity to 5–7 cm/yr, the temperature contrast will only increase by about 100°C, corresponding to a 0.04–0.06 km/s ($\sim 0.6\%$) change in $V_p$. Thus, with an initial $V_p$ of 7.8–8.0 km/s at depths of 50–100 km, an increase of $V_p$ to 8.3 km/s can easily be achieved.

In the thermal model described above, the calculated temperature of the mantle wedge has an average value of about 100°C less than the ''normal mantle'' at depths of 50 to 100 km, corresponding to a 0.04–0.06 km/s change in $V_p$. This small amount of change in $V_p$ cannot explain the observations (0.4–0.6 km/s changes in $V_p$) in the mantle wedge. In addition to the temperature contrast that lowers the $V_p$ slightly, we must consider the effects of partial melting and water on $V_p$ in the mantle wedge. For the effect of partial melt on $V_p$, 3–5% melt proportions are required for 0.4–0.6 km/s changes in $V_p$ in the mantle wedge [28]; the exact amount is not resolvable because of the dependence of melt fraction on the morphology of the melts. For the effect of water on $V_p$, Ito [33] found that, at a pressure of 10 kbar and a temperature of 900°C, 5% drop of $V_p$ can be explained by the presence of about 20 kg/m$^3$ water in the mantle rocks; the free water can be released by dehydration of the hydrous minerals derived from subducting slab [34]. Either one of these two factors provides a possible explanation to a lowered $V_p$ in the mantle wedge.

## 5. Conclusion

Using seismic arrival time data accumulated in three and a half years, from the telemetered seismic network in Taiwan, clear images of velocity distributions in the crust and upper mantle under Taiwan have been obtained. The subduction zone under northern Taiwan was delineated and so was the low-velocity mantle wedge above it. Based on these results we are able to delineate the location of the ''trench'' for the subduction zone offshore of northern Taiwan and place a part of northern Taiwan above the low-velocity wedge. Also clearly shown in the images are the thickening of the crust under the Central Range and the presence of high-velocity materials at shallow depth under the Central Range. The extent of thickening decreases from Hualien southward as the mountain range becomes younger. If our interpretation is correct, it implies that the mountain building in Taiwan involves the participation of crust and upper mantle and it calls into question the appropriateness of the modeling of Taiwan orogeny in terms of thin-skinned tectonics.


## Acknowledgements

We are grateful to Clifford H. Thurber, Donna Eberhart-Phillips, and Bill Ellsworth for providing their computer programs, to Ban-Yuan Kuo for discussions and assistance in computing temperature profiles, and to Wang-Ping Chen for many helpful comments on the manuscript. We also thank T.C. Shin and the staffs in the Central Weather Bureau Seismological Observation Center of Taiwan, ROC, for providing and discussing the earthquake data. Figures used in this study were generated from GMT-SYSTEM v. 2.1.4 [35]. Computations were done on the NSF/SUNY-funded SUN workstations. The text benefited from the constructive reviews of Chi-yuen Wang, Dapeng Zhao and Charles Langmuir. This research was supported by grant EAR-9206545 from the National Science Foundation. [CL]




## References


[1] F.T. Wu, Recent tectonics of Taiwan, J. Phys. Earth 26(suppl.), S265–S299, 1978.

[2] R.J. Rau, Flexure modeling and Taiwan tectonics, Thesis, 131 pp, State Univ. New York, Binghamton, NY, 1992.

[3] T. Seno, S. Stein and A.E. Gripp, A model for the motion of the Philippine Sea plate consistent with NUVEL-1 and geological data, J. Geophys. Res. 98, 17,941–17,948, 1993.

[4] S. Tsao, T.C. Li, J.L. Tien, C.H. Chen, T.K. Liu and C.H. Chen, Illite crystallinity and fission-track ages along the east central cross-island highway of Taiwan, Acta Geol. Taiwan. 30, 45–64, 1992.

[5] S.B. Yu, D.D. Jackson, G.K. Yu and C.C. Liu, Dislocation model for crustal deformation in the Longitudinal Valley area, eastern Taiwan, Tectonophysics 183, 97–109, 1990.

[6] J. Suppe, Mechanics of mountain building in Taiwan, Mem. Geol. Soc. China 4, 67–89, 1981.

[7] S.W. Roecker, Y.H. Yeh and Y.B. Tsai, Three-dimensional P and S wave velocity structures beneath Taiwan: deep structure beneath an arc–continent collision, J. Geophys. Res. 92, 10,547–10,570, 1987.

[8] Y.H. Yeh, C.H. Lin and S.W. Roecker, A study of upper crustal structures beneath northeastern Taiwan: possible evidence for the western extension of Okinawa trough, Proc. Geol. Soc. China 32, 139–156, 1989.

[9] T.Q. Lee, C. Kissel, E. Barrier, C. Laj and W.R. Chi, Paleomagnetic evidence for a diachronic clockwise rotation of the Coastal Range, eastern Taiwan, Earth Planet. Sci. Lett. 104, 245–257, 1991.

[10] C.H. Thurber, Earthquake locations and three-dimension crustal structure in the Coyote Lake area, central California, J. Geophys. Res. 88, 8226–8236, 1983.

[11] C.H. Thurber, Local earthquake tomography: Velocities and $V_p/V_s$-Theory, in: Seismic Tomography: Theory and Practice, H.M. Iyer and K. Hirahara, eds., pp. 563–583, Chapman and Hall, London, 1993.

[12] J. Suppe, The active Taiwan mountain belt, in: The Anatomy of Mountain Ranges, J.P. Schaer and J. Rodgers, eds., pp. 277–293, Princeton Univ. Press, Princeton, NJ, 1987.
[13] W.L. Ellsworth, Three-dimensional structure of the crust and mantle beneath the island of Hawaii, Ph.D. thesis, 237 pp., Mass. Inst. Technol., Cambridge, MA, 1977.
[14] D. Eberhart-Phillips, Local earthquake tomography: earthquake source regions, in: Seismic Tomography: Theory and Practice, H.M. Iyer and K. Hirahara, eds., pp. 614–643, Chapman and Hall, London, 1993.
[15] G.L. Pavlis and J.R. Booker, The mixed discrete–continuous inversion problem: application to the simultaneous determination of earthquake hypocenters and velocity structure, J. Geophys. Res. 85, 4801–4810, 1980.
[16] J. Um and C.H. Thurber, A fast algorithm for two-point seismic ray tracing, Bull. Seismol. Soc. Am. 77, 972–986, 1987.
[17] W. Menke, Geophysical Data Analysis: Discrete Inverse Theory, 289 pp., Academic Press, New York, NY, 1989.
[18] D.R. Toomey and G.R. Foulger, Tomographic inversion of local earthquake data from the Hengill-Grensdalur central volcano complex, J. Geophys. Res. 94, 17,497–17,510, 1989.
[19] C.H. Thurber, Earth structure and earthquake locations in the Coyote Lake area, central California, Ph.D. thesis, 332 pp., Mass. Inst. Technol., Cambridge, MA, 1981.
[20] H. Chen, Crustal uplift and subsidence in Taiwan; an account based upon retriangulation results, Spec. Publ. Cent. Geol. Surv. 3, 127–140, 1984.
[21] R. van der Hilst, R. Engdahl, W. Spakman and G. Nolet, Tomographic imaging of subducted lithosphere below northwest Pacific island arcs, Nature 353, 37–43, 1991.
[22] E. Kissling and J.C. Lahr, Tomographic image of the Pacific slab under southern Alaska, Eclogae Geol. Helv. 84(2), 297–315, 1991.
[23] D. Zhao, A. Hasegawa and H. Kanamori, Deep structure of Japan subduction zone as derived from local, regional, and teleseismic events, J. Geophys. Res. 99, 22,313–22,329, 1994.
[24] J.F. Stephan, R. Blanchet, C. Rangin, B. Pelletier, J. Letouzey and C. Muller, Geodynamic evolution of the Taiwan–Luzon–Mindoro belt since the late Eocene, Mem. Geol. Soc. China 7, 69–90, 1986.
[25] J. Suppe, Kinematics of arc–continent collision, flipping of subduction, and back-arc spreading near Taiwan, Mem. Geol. Soc. China 6, 21–34, 1984.
[26] T.H. Jordan, Composition and development of the continental tectosphere, Nature 274, 544–548, 1978.
[27] T.H. Jordan, Mineralogies, densities and seismic velocities of garnet lherzolites and their geophysical implications, in: The Mantle Sample: Inclusions in Kimberlites and Other Volcanics, F.R. Boyd and H.O.A. Meyer, eds., pp. 1–14, Am. Geophys. Union, Washington, DC, 1979.
[28] G.R. Helffrich, S. Stein and B.J. Wood, Subduction zone thermal structure and mineralogy and their relationship to seismic wave reflections and conversions at the slab/mantle interface, J. Geophys. Res. 94, 753–763, 1989.
[29] H. Kern, P-and S-wave velocities in crustal and mantle rocks under the simultaneous action of high confining pressure and high temperature and the effect of the rock microstructure, in: High-Pressure Researches in Geoscience, W. Schreyer, ed., pp. 15–45, Schweizerbart, Stuttgart, 1982.
[30] D.M. Fountain and N.I. Christensen, Composition of the continental crust and upper mantle; a review, Geol. Soc. Am. Mem. 172, 711–742, 1989.
[31] N.I. Christensen, Compressional wave velocities in possible mantle rocks to pressures of 30 kilobars, J. Geophys. Res. 79, 407–412, 1974.
[32] K.C. Creager and T.H. Jordan, Slab penetration into the lower mantle beneath the Mariana and other island arcs of the northwest Pacific, J. Geophys. Res. 91, 3573–3589, 1986.
[33] K. Ito, Effects of $H_2O$ on elastic wave velocities in ultrabasic rocks at 900°C under 1 Gpa, Phys. Earth Planet. Inter. 61, 260–268, 1990.
[34] Y. Tatsumi, Migration of fluid phases and genesis of basalt magmas in subduction zones, J. Geophys. Res. 94, 4697–4707, 1989.
[35] P. Wessel and W.H.F. Smith, Free software helps map and display data, EOS Trans. Am. Geophys. Union 72, 441, 1991.


*1. Submission of manuscripts*

Contributions may be sent directly to one of the editors or through the intermediary of one of the members of the Advisory Editorial Board. Four copies of the manuscript including photographs, line-drawings and tables should be submitted. Original line-drawings should *not* be sent until the final revised manuscript is submitted to the editor. Submission of an article is understood to imply that the article is original and unpublished and is not being considered for publication elsewhere. With the submitted manuscript, authors should enclose the names and addresses of five suggested reviewers. The editors will keep the identity of the reviewers anonymous but the reviewers may feel free to correspond directly with the authors if they so desire. The responsibility for direct communication between the reviewer and the author must lie with the reviewer. **With a view to increasing the speed of publication authors are encouraged to revise within 6 weeks after receiving their reviews. At the editors' discretion, any revision received after this time limit may be regarded as a new submission that is subject to handling as a new paper.** Upon acceptance of an article by the journal, the author(s) will be asked to transfer the copyright of the article to the publisher. This transfer will ensure the widest possible dissemination of information. **There is an "Express Letter Section" for short, original papers. The maximum permissible length is 5 journal pages and the total time from submission to publication will be ca. 3 months. Please refer to the announcement in this issue for more details.** (a) *Submission of electronic text* In order to publish the paper as quickly as possible, after acceptance* authors are encouraged to submit the final text also on a diskette. Please see the full instructions in the last issue of this volume. **Authors are encouraged to ensure that the diskette version and the hardcopy are identical — discrepancies can lead to publication of the wrong version. *Only the title page and abstract should be provided on diskette with the original submission; this will be used when e-mailing potential referees.**

*2. Length of papers*

THE MAXIMUM PERMISSIBLE LENGTH OF PAPERS IS 15 PRINTED JOURNAL PAGES. A WORD COUNT MUST BE PROVIDED ON THE TITLE PAGE OF MANUSCRIPTS. THERE ARE NO PAGE CHARGES.

*3. Language*

Manuscripts should be written in English only, and except for very short papers they should include a brief abstract.

*4. Preparation of the text*

(a) The manuscript should be prepared on a word processor and printed with double spacing and wide margins and include an abstract of not more than 500 words.
(b) Authors should use IUGS terminology. The use of S.I. units is also recommended.
(c) The title page should include the names of the authors, and their affiliation addresses and fax and e-mail numbers. In the case of more than one author, please indicate to whom the correspondence should be addressed.

*5. References*

References should be limited to the minimum number necessary for citation of pertinent material. As a guide an average of 4 references per printed page can be used, **with a maximum of 50 references per article.** References to internal reports, etc., are to be avoided (The statement "personal communication" with publication date in the text is preferable.)
References to the literature should strictly follow the journal's format: the references should be numbered in the order in which they are cited, and given in numerical sequence in the reference list at the end of the manuscript. The numbers should appear in the text in the appropriate places using numerals in square brackets on the line. In the reference list, periodicals [1], books [2], multi-author books [3] and proceedings [4], should be cited in accordance with the following examples:

1 I.M. Villa, J.C. Huneke and G.J. Wasserburg, "Ar recoil losses and presolar ages in Allende inclusions, Earth Planet. Sci. Lett. 63, 1–12, 1983.
2 I.S.E. Carmichael, F.J. Turner and J. Verhoogen, Igneous Petrology, 739 pp., McGraw-Hill, New York, N.Y., 1974.
3 S.R. Taylor, Chemical composition and evolution of the continental crust: the rare earth element evidence, in: The Earth, its Origin, Structure and Evolution, M.W. McElhinney, ed., pp. 2–44, Academic Press, London, 1978.
4 V.T. Bowen, H.D. Livingston and J.C. Burke, Distribution of transuranium nuclides in sediment and biota of the North Atlantic Ocean, in: Transuranium Elements in the Environment, IAEA Symp. Proc., pp. 107–120, 1976.

Abbreviations for titles of journals should follow the system used in the "Bibliographic Guide for Editors and Authors" published in 1974 by the American Chemical Society, Washington, D.C.

*6. Tables and illustrations*

Tables should be compiled on separate sheets. A title should be provided for each table and they should be referred to in the text. Tables can also be sent as camera-ready versions to avoid errors in type-setting; a normal page-size reproduction of such tables should also be included in the manuscript. Efforts should be made to make the size of the tables correspond to the format of the journal (max. 15×20 cm).

(a) All illustrations should be numbered consecutively and referred to in the text.
(b) Illustrations should be lettered throughout, the size of the lettering being appropriate to that of the illustrations, but taking into acount the possible need for reduction in size. The page format of the journal should be considered in designing the illustrations. All illustrations must be originals, in the form of glossy figures or laser prints. Each illustration must be accompanied by a photocopy.
(c) Photographs must be of good quality, printed on glossy paper.
(d) Figure captions should be supplied on a separate sheet.
(e) Colour figures can be accepted providing the reproduction costs are met by the author. Please consult the publisher for further information.

*7. Proofs*

To achieve the high speed of publication, no proofs are sent to the authors. Manuscripts should therefore be prepared with the greatest possible care, and the submission of negatives for tabular material is encouraged. Galley proofs may occasionally be obtained by making a special request to the editor, with the understanding that this implies delay in publication.

*8. Fifty free reprints*

Fifty reprints of each article published are supplied free of charge. A form for ordering extra reprints will be sent to the corresponding author on receipt of the accepted manuscript by the publisher.